

**STRUCTURAL DESIGN AND ANALYSIS OF A LIGHTWEIGHT
COMPOSITE SANDWICH SPACE RADIATOR PANEL**

A Thesis

by

SUDHARSAN MUKUNDAN

Submitted to the Office of Graduate Studies of
Texas A&M University
in partial fulfillment of the requirements for the degree of

MASTER OF SCIENCE

December 2003

Major Subject: Mechanical Engineering

**STRUCTURAL DESIGN AND ANALYSIS OF A LIGHTWEIGHT
COMPOSITE SANDWICH SPACE RADIATOR PANEL**

A Thesis

by

SUDHARSAN MUKUNDAN

Submitted to Texas A&M University
in partial fulfillment of the requirements
for the degree of

MASTER OF SCIENCE

Approved as to style and content by:

Ozden O. Ochoa
(Chair of Committee)

David R. Boyle
(Member)

Reza Langari
(Member)

Dennis L. O'Neal
(Interim Head of Department)

December 2003

Major Subject: Mechanical Engineering

ABSTRACT

Structural Design and Analysis of a Lightweight Composite Sandwich Space Radiator

Panel. (December 2003)

Sudharsan Mukundan, B.E., Bharathiar University, Coimbatore, India

Chair of Advisory Committee: Dr. Ozden O.Ochoa

The goal of this study is to design and analyze a sandwich composite panel with lightweight graphite foam core and carbon epoxy face sheets that can function as a radiator for the given payload in a satellite. This arrangement provides a lightweight, structurally efficient structure to dissipate the heat from the electronics box to the surroundings. Three-dimensional finite element analysis with MSC Visual Nastran is undertaken for modal, dynamic and heat transfer analysis to design a radiator panel that can sustain fundamental frequency greater than 100 Hz and dissipate 100 W/m² and withstand launch loads of 10G.

The primary focus of this research is to evaluate newly introduced graphite foam by Poco Graphite Inc. as a core in a sandwich structure that can satisfy structural and thermal design requirements. The panel is a rectangular plate with a cutout that can hold the antenna. The panel is fixed on all the sides. The objective is not only to select an optimum design configuration for the face sheets and core but also to explore the potential of the Poco foam core in its heat transfer capacity. Furthermore the effects of various parameters such as face sheet lay-up, orientation, thickness and material properties are studied through analytical models to validate the predictions of finite element analysis. The optimum dimensions of the sandwich panel are determined and structural and thermal response of the Poco foam is compared with existing aluminum honeycomb core.

ACKNOWLEDGEMENTS

Above all I would like to thank the almighty for his continued blessings that have helped me complete this work successfully.

I wish to express my sincere gratitude to my committee chair, Dr. Ozden Ochoa, for guiding this project and making me realize the importance of perfection and quality. I also like to thank her for her continued support, morally and academically.

I am thankful to Ms. Magdalini Lagoudas, for supporting me throughout this project and providing valid timely ideas and suggestions. Without her patience and constant motivation, this thesis would never have been completed. I would also like to thank her for supporting me financially for this project. Her emphasis on time and management of work made me a better professional.

I would like to express my gratitude to Dr. David Boyle, Director, Spacecraft Technology Center, for providing financial support throughout my graduate education. I would also like to thank him for serving as a committee member and allocating valuable time amidst his busy schedule.

I am thankful to Mr. Olivier Godard for being a nice mentor and friend. His support and timely help contributed towards the completion of the project

I am thankful to Dr. Reza Langari for agreeing to serve on my graduate committee and providing valuable time.

My sincere thanks to the staff members of the Spacecraft Technology Center for providing me a supportive environment for this research work. My appreciation also goes to the Department of Mechanical Engineering for their patience and kind help in the course of my graduate study.

I would like to thank my friend, Deepak Goyal, who has provided valuable suggestions in improving the quality of this work. My heartfelt thanks go to all the people who have indirectly contributed toward the completion of my thesis.

Last, but not the least, I would like to acknowledge my parents and sister for their patience, understanding, love and affection without which my graduate education on a foreign soil would have been difficult.

TABLE OF CONTENTS

	Page
ABSTRACT.....	iii
ACKNOWLEDGEMENTS.....	iv
TABLE OF CONTENTS.....	vi
LIST OF TABLES.....	ix
LIST OF FIGURES.....	x
CHAPTER	
I. INTRODUCTION.....	1
1.1 Rationale.....	2
1.2 Problem Description.....	2
1.3 Approach.....	3
II. BACKGROUND.....	5
2.1 Sandwich.....	5
2.1.1 Face Sheets.....	6
2.1.2 Cores.....	6
2.1.2.1 Aluminum Honeycomb.....	7
2.1.2.2 Carbon and Graphite Foams.....	7
2.2 Design Considerations in Sandwich Construction.....	10
2.2.1 Structural Considerations.....	10
2.2.2 Environmental Considerations.....	10
2.3 Failure Modes of Sandwich Structures.....	11
2.4 Stress Distribution in Sandwich Beam.....	13
2.5 Literature Review.....	14
III. FINITE ELEMENT MODELING OF SANDWICH PANEL.....	18
3.1 Material Definition.....	18
3.2 Element Types.....	21
3.2.1 2D Laminate Element.....	21
3.2.2 3D Solid Element.....	22
3.3 Modeling Classification.....	23
3.3.1 Shell/Shell Representation.....	23
3.3.2 Shell/Solid Representation.....	24
3.3.3 Solid/Solid Representation.....	24
3.3.4 Defining the Layers and Stacking Sequence.....	24
3.4 Material Properties.....	25
3.4.1 Face Sheet.....	25
3.4.2 Core.....	27

	Page
5.3 Static and Dynamic Analysis Results of Radiator Panel.....	85
5.3.1 Dynamic Load Sets.....	85
5.3.2 Stress Distribution.....	87
5.4 Heat Transfer Analysis of Radiator Panel.....	89
5.4.1 Temperature Distribution.....	91
5.4.2 Thermal Stress Distribution.....	93
5.4.3 Transient Heat Transfer Analysis.....	95
5.4.4 Orbit Analysis Results.....	98
5.4.5 Electronics Box Approach.....	100
5.5 Conclusion.....	104
REFERENCES.....	105
APPENDIX 1.....	108
APPENDIX 2.....	110
APPENDIX 3.....	111
VITA.....	113

LIST OF TABLES

	Page
Table 3.1. Material properties of sandwich cores.....	30
Table 4.1. Non-dimensional fundamental frequency for sandwich plate.....	43
Table 4.2. Elastic properties of T300/5208 carbon epoxy.....	45
Table 4.3. Random vibration load set calculation for radiator panel.....	55
Table 5.1. Modal comparison between MSC Nastran and analytical solution.....	77
Table 5.2. Modal results of sandwich panel with different types of core.....	78
Table 5.3. Fundamental frequencies of cross ply lay-ups for radiator panel.....	80
Table 5.4. Fundamental frequencies of angle ply lay-ups for radiator panel.....	81
Table 5.5. Fundamental frequencies of the optimized radiator sandwich panel.....	83
Table 5.6. Dynamic loads for sandwich panel with Poco foam as core.....	85
Table 5.7. Dynamic loads for sandwich panel with Poco foam HTC as core.....	86
Table 5.8. Dynamic loads for sandwich panel with aluminum honeycomb as core.....	86
Table 5.9. Stress distribution summary.....	89
Table 5.10. Steady state temperature distribution in the radiator panel.....	93
Table 5.11. Thermal stress field in the radiator panel.....	94
Table 5.12. Thermal stress comparison with laminator.....	95
Table 5.13. Transient analysis data for different core materials.....	97
Table 5.14. Orbit analysis temperature at the core.....	99
Table 5.15. Steady state temperature of the electronics box.....	103

LIST OF FIGURES

	Page
Figure 1.1. Payload with radiator panel and electronics box.....	3
Figure 2.1. Typical geometry of sandwich panel.....	6
Figure 2.2. Highly graphitic microstructure of Poco foam.....	9
Figure 2.3. Tensile fracture of face sheets of sandwich	11
Figure 2.4. Face sheet wrinkling.....	12
Figure 2.5. Shear failure in the core.....	12
Figure 2.6. Debonding phenomena.....	12
Figure 2.7. Approximate stress distribution in a sandwich beam.....	13
Figure 3.1. Orthotropic 2D material definition.....	19
Figure 3.2. Anisotropic 2D material definition.....	19
Figure 3.3. Orthotropic 3D material definition.....	20
Figure 3.4. Anisotropic 3D material definition.....	21
Figure 3.5. 2D laminate type element.....	22
Figure 3.6. Typical eight noded solid element.....	22
Figure 3.7. Material data form of face sheet T300/5208 carbon epoxy [0].....	27
Figure 3.8. Sandwich panel model with face sheets and core (MSC Nastran).....	32
Figure 3.9. Sandwich radiator panel with antenna at the cutout.....	34
Figure 4.1. The variation of the fundamental frequency with the thickness of the isotropic plate.....	39
Figure 4.2. The variation of the fundamental frequency with the thickness of the core (h_c) (keeping the thickness of the face sheet (t_f) as constant).....	43
Figure 4.3. The variation of the non-dimensional frequency with the parameter R ($R=h_c/t_f$).....	44
Figure 4.4. The variation of the non-dimensional frequency with the face sheet thicknesses (t_{f1} and t_{f2}). (Core thickness (h_c) is constant).....	44
Figure 4.5. Edge constraints of sandwich radiator panel.....	47
Figure 4.6. Power spectral density levels.....	54

	Page
Figure 4.7. Dynamic load set for radiator panel.....	56
Figure 4.8. Schematic representation of the heat removal system from the electronics box.....	58
Figure 4.9. Schematic representation of heat loads modeled in MSC Nastran.....	59
Figure 4.10. MSC Nastran units for heat loads.....	61
Figure 4.11. Nodal heat load form in MSC Nastran.....	62
Figure 4.12. Sandwich panel with heat flux and radiation (MSC Nastran).....	63
Figure 4.13. One-dimensional analytical model for temperature field.....	64
Figure 4.14. Transient analysis form in MSC Nastran.....	71
Figure 5.1. Isotropic plate.....	76
Figure 5.2. Specially orthotropic laminate [0/90/90/0].....	76
Figure 5.3. Sandwich plate [0/90/core/90/0].....	76
Figure 5.4. Fundamental mode shape of the Poco foam sandwich radiator panel.....	84
Figure 5.5. VonMises stress distribution of face sheet [0] for launch load set 3.....	87
Figure 5.6. VonMises stress distribution of face sheet [90] for launch load set 3.....	88
Figure 5.7. VonMises stress distribution of Poco foam core for launch load set 3.....	88
Figure 5.8. VonMises stress distribution of honeycomb core for launch load set 3.....	89
Figure 5.9. Temperature distribution of Poco foam core.....	91
Figure 5.10. Temperature distribution of face sheet [0] exposed to radiation.....	91
Figure 5.11. Temperature distribution of aluminum honeycomb core.....	92
Figure 5.12. Transient temperature plot of a node in core for non-optimized panel from MSC Nastran.....	96
Figure 5.13. Transient temperature plot of core for optimized panel (assuming no face sheets).....	98
Figure 5.14. Material data form for beryllium copper alloy.....	101
Figure 5.15. Electronics box model set up in MSC Nastran.....	101
Figure 5.16. Model of electronics box approach with heat generation and radiation.....	102
Figure 5.17. Time –temperature plot for a node of the electronics box.....	103

CHAPTER I

INTRODUCTION

Composite materials, due to their high specific thermal, stiffness and strength properties, have always been enabling systems for spacecraft applications. They are excellent candidates for radiators for space borne electronic systems in order to reduce overall weight and to dissipate the heat rapidly from the source to the surrounding space. The trend for future satellites is compact packaging of electronic gadgets where heat removal must be rapid. The aim is to build spacecrafts with high power density combined with reduction in size and weight. Since spacecraft applications demand low weight, high stiffness to weight ratio and high structural stability, sandwich panels with composite face sheets and a lightweight core are likely candidates to be used as spacecraft radiators. Earlier aluminum plates were used as heat sinks for many printed circuit board assemblies in space flight applications [1]. These plates also served as structural support providing the necessary in-plane stiffness in order to survive the vibration environment during spacecraft launch. Owing to the higher specific thermal conductivity and stiffness of composites than aluminum, sandwich composite panel have started replacing aluminum in spacecraft thermal management issues.

Designing lightweight radiators or heat sinks has become increasingly important as payload weight increases more and more during each launch. Lightweight composite materials and foams can replace the aluminum radiators, which are heavy. Another significant advantage of replacing aluminum by lightweight composite materials is the reduction of the thermal stresses due to low coefficient of thermal expansion of carbon/graphite foams. A special class of composite materials called the carbon-carbon composites, with low density and high thermal conductivity, is specifically suited to radiators as it offers improved performance for lower volume and mass [2].

This thesis follows the style and format of Composite Structures.

The carbon-carbon composite radiator along with aluminum honeycomb core spreads heat across a larger surface area and reduces temperature of the electronics. But due to low through the thickness thermal conductivity of current carbon-carbon face sheet and aluminum honeycomb core, the panel restricts the amount of heat rejected to space in unit time. However high conductivity carbon/graphite foams as cores in sandwich panels, offers an increase in through the thickness thermal conductivity. This increases the heat dissipated to space as it is dissipated with ΔT^4 relationship.

1.1 Rationale

The recent successful processing of high thermal conductivity carbon and graphite foams has stimulated interest in implementing these foams separately or as cores in sandwich panels with composite face sheets for thermal management applications such as radiators, batteries and electronic packaging. In addition, the heat generated from electronic devices during space flight operation, is a functional constraint and hence improved thermal management using lightweight graphite foams potentially may lead to better system performance.

This thesis investigates the potential performance merits of using Poco graphite foam [3] as a core in a composite sandwich panel that will function as a radiator for the payload. The panel is analyzed for launch loads and heat transfer capabilities using the software MSC Visual Nastran for windows 2002 [4]. If the proposed design proves successful there could be a significant change in the construction of the radiators for future spacecraft and could lead to significant cost and weight reduction.

1.2 Problem Description

The radiator is a sandwich rectangular panel constrained on all the edges as it is secured at the top of the structure as shown in the Figure 1.1. The panel has composite face

sheets and a lightweight foam core. The panel contains a central cutout to hold the antenna. The design requirements are to have fundamental frequency greater than 100 Hz, to dissipate 100 Watts/m² of heat flux and withstand dynamic launch loads. The objective of this design is to select an optimum configuration that satisfies the above design requirements.

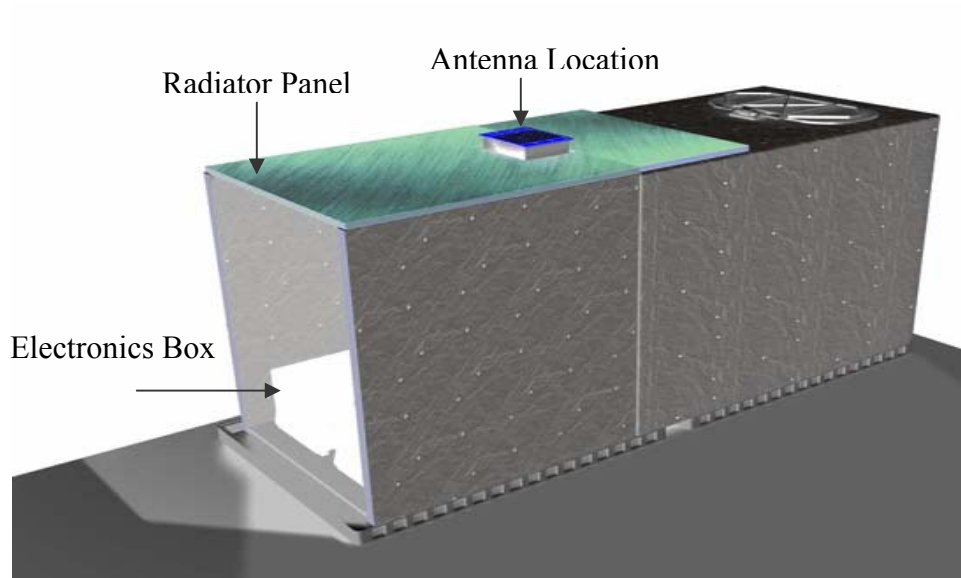


Figure 1.1. Payload with radiator panel and electronics box.

1.3 Approach

Three-dimensional finite element analysis of the sandwich panel is conducted with solid elements, implemented in MSC Visual Nastran for Windows 2002. With the given boundary condition, the sandwich panel is subjected to vibration, gravitational and thermal loads to predict the modes and stresses in the sandwich panel. The design is sequential starting with structural requirements and then gravitational followed by thermal simulations.

The parameters such as thickness of face sheets, core and their material properties are chosen to provide sufficient structural stiffness so that the fundamental frequency is more than 100 Hz. Then the analysis involves the application of launch loads on the panel to study the structural response and to ensure that the structural integrity is maintained. The stress characteristics are predicted on all the individual layers of the sandwich. The selected configuration of the sandwich panel is then analyzed by supplying heat flux of 100 W/m^2 to the mid-plane of the core and allowing it to radiate to only one side. Finally a design methodology with the optimum core, facesheet parameters, is proposed to minimize the temperature of the electronics in the spacecraft.

CHAPTER II

BACKGROUND

2.1 Sandwich

Composite materials consist of two or more constituent materials whose properties can be tailored to create unique mechanical, material and physical response for a variety of applications. Fiber-reinforced composite materials consist of high strength and or high modulus fibers that are the principal load carrying members and the matrix acts as a load transfer medium between the fibers.

Sandwich [5] structures (beams, panels etc.) consist of a combination of different materials that are placed together so that the material properties of each one can be utilized for the structural advantage of the whole assembly. Sandwich panels generally consist of three significant components, two thin, stiff face sheets and a thick, light and weaker core. The bending stiffness and stiffness to weight ratio of the sandwich is greater than a single solid plate of same total weight and same material as that of the faces. As a result sandwich construction results in lower lateral deformations, higher buckling resistance and higher natural frequencies than do other constructions.

The design principle of a sandwich composite is similar to that of an I-beam, which is an efficient structural shape because as much as possible of the material is placed in the flanges situated farthest from the center of bending and neutral axis. In a sandwich, the faces resemble the flanges and the core acts as the web. The faces act together to form an efficient stress couple or resisting moment, counteracting the external bending moment. The core resists shear and stabilize the faces against buckling or wrinkling. The selection of the adhesive that bonds the faces to the core is of critical importance as it must be strong enough to resist the shear and tensile stresses set up between them. Typical sandwich [6] geometry is shown in the Figure 2.1.

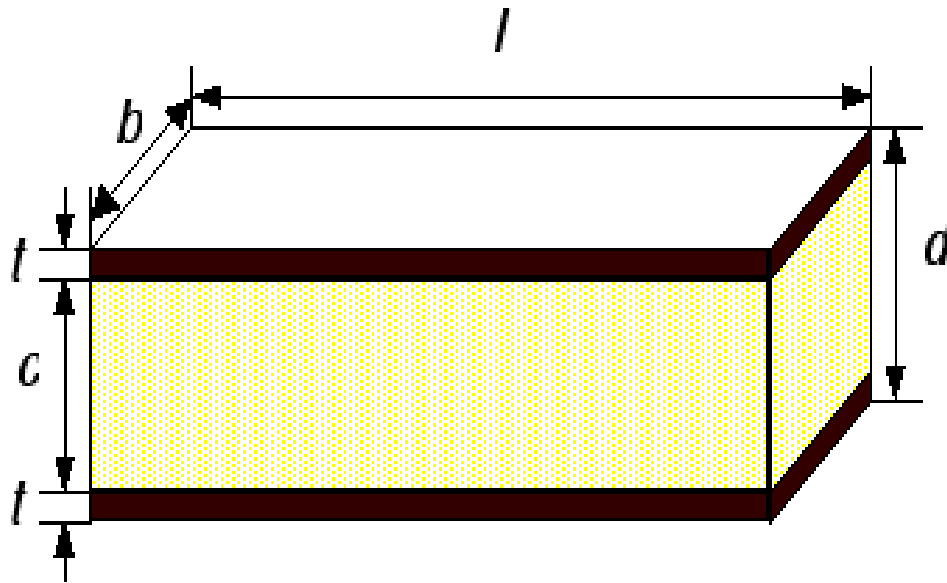


Figure 2.1. Typical geometry of sandwich panel.

2.1.1 Face sheets

The face sheets provide the flexural rigidity of the sandwich panel. It should also possess tensile and compressive strength. Since the carbon-epoxy composite has lower density than aluminum, significant weight savings can be realized by replacing them. The analysis of composite plates by Harris et al. [7] indicates that the sandwich plates with carbon epoxy face sheets have the lowest weight for different loading cases and that they are dimensionally more stable for a wide range of temperatures.

2.1.2 Cores

The purpose of the core is to increase the flexural stiffness of the panel. The core in general has low density in order to add as little as possible to the total weight of the sandwich construction. The core must be stiff enough in shear and perpendicular to the faces to ensure that face sheets are distant apart. In addition the core must withstand compressive loads without failure. The cores can be almost any material, but in general fall into the following four types. They are foam or solid core, honeycomb core, Web

core and Corrugated or truss core. In Web core and truss core construction, a portion of the in-pane and bending loads are also carried by the core elements.

2.1.2.1 Aluminum Honeycomb

They are available in variety of materials for sandwich structures. They range from low strength and stiffness applications to high strength and lightweight applications such as aircraft industries. They can be formed to any shape or curve without excessive heating or mechanical force. Honeycombs have very high stiffness perpendicular to the faces and the highest shear stiffness and strength to weight ratios of the available core materials. The most commonly used honeycombs are made of aluminum or impregnated glass or aramid fiber mats such as Nomex and thermoplastic honeycombs. The main drawback is high cost and difficulty in handling.

Honeycombs are generally produced by extrusion followed by slicing to thickness. The slices are then gently stretched and expanded to form a sheet of continuous hexagonal cell shapes. Due to the bonded method of construction and due to the varying degree of pull, these hexagonal cells have different properties in the 0^0 and 90^0 directions of the material. The cells of the honeycomb structure can also be filled with rigid foams to increase the rigidity and thermal insulation of the foam. This also increases the bond area of the skins to the core. The most common types of honeycomb are Aluminum Honeycomb, Nomex Honeycomb and Thermoplastic honeycomb.

2.1.2.2 Carbon and Graphite Foams

Carbon foam is the enabling technology for a host of next generation products and components replacing the conventional materials from its use. High thermally conductive carbon foams were first reported in 1998 at Oak Ridge National Laboratory

[8] and are currently being developed for variety of uses including fire resistant ship decks and hulls, noise and impact mitigation for aircrafts, structural panels, thermal doublers, radiators for sport cars and spacecraft thermal management systems.

Graphite foams are generally formed by heat-treating carbon foam to more than 2000⁰C. This patented ORNL method for making the special graphite foam was licensed to Poco Graphite Inc., Decatur, Texas. Poco graphite Foam is a lightweight material that has exceptionally high thermal conductivity in through the thickness direction. It has 3 to 9 times higher thermal conductivity than typical carbon foams and 10 times higher than metallic aluminum foam. Poco foam is derived from mesophase pitch, an intermediate phase in the formation of carbon and when heated above 2000⁰C forms graphite. The reason for its exceptionally high thermal conductivity is that the precursor material combined with an efficient production method makes the ligaments, which are like honeycomb structure, a highly aligned graphitic nature rather than an amorphous one.

It is known that decreasing the density of the material by foaming decreases thermal conductivity. Graphite has a layered structure that has a strong bond between the hexagonal carbon atoms in the plane but has only a weak bond between the planes. Therefore the thermal conductivity is extremely high in the plane but poor through the thickness. The graphite foams are derived from mesophase pitch precursor in which, the mesophase crystals align themselves along the cell walls as shown in Figure 2.2. This foam when graphitized at high temperatures of 2800⁰C becomes highly aligned and defect free graphite structure. Pure graphite exhibits 1800 W/m-K along the X and Y axis of its planes but less than 5 W/m-K along the Z-axis [9]. Therefore foaming the graphite to about 25% density makes the material more isotropic by reorienting the hexagonal carbon atoms into spherical structures as they form the individual cell walls. As a result the conductivity drops to about 90 W/m-K along the X and Y-axis but soars to 150 W/m-K along the Z-axis.

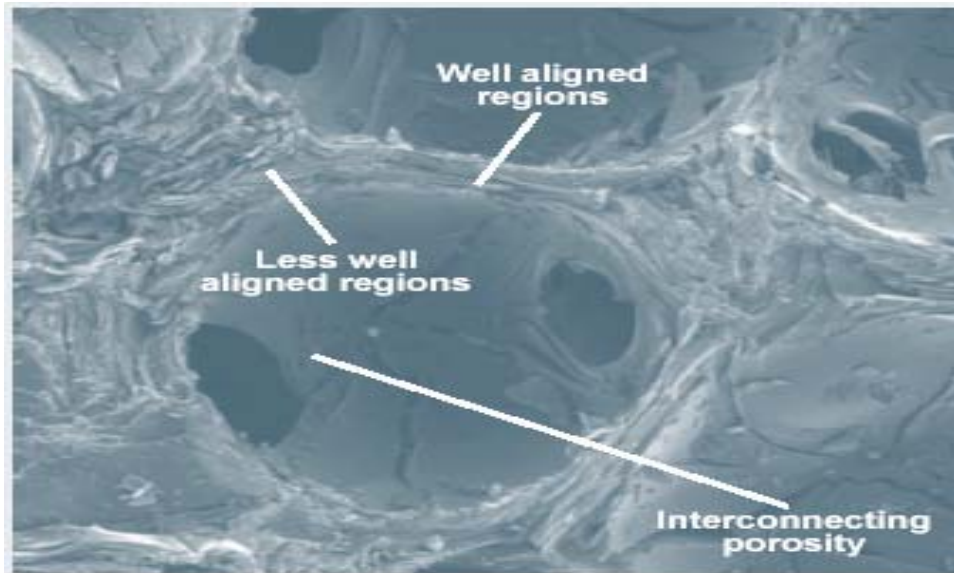


Figure 2.2. Highly graphitic microstructure of Poco foam. [8]

Poco foam differs from conventional carbon foams in the sense that the ligaments are of a highly aligned graphitic nature rather than an amorphous one. This difference in its structure gives high dimensional stability, low coefficient of thermal expansion, relatively high modulus of elasticity and exceptionally high thermal conductivity. Due to its porous nature and high internal surface area, it has efficient heat transfer characteristics. It has high thermal diffusivity i.e. the ability to transport the heat quickly compared to absorbing the heat. Thus its low density, open porosity and high thermal characteristics make it a promising material for thermal management applications.

- The density of the Poco foam is 0.55 g/cm^3 , which is 6% of copper and 20% of aluminum.
- The Poco foam is three to nine times more thermally conductive than carbon foams ($0.25 - 70 \text{ W/m}^0\text{K}$)
- The specific thermal conductivity of Poco foam is around 272 W/m-K in the out of plane direction and it is six times greater than copper and five times greater than aluminum.

2.2 Design Considerations in Sandwich Construction

There are many plausible core and face sheet materials that can be selected for the sandwich construction. The components of the sandwich are bonded together using adhesives or mechanical fastenings such that they can act as a composite load bearing unit. The basic underlying concept of sandwich is that face sheets carry the bending stresses and the cores carry the shear stresses. The bending stiffness of the sandwich is very much higher than a solid structure having the same total weight and the same material as the facings.

2.2.1 Structural Considerations

As properties of honeycomb cores and face sheet materials are directional, it is vital to make sure that the materials are oriented along the optimum axis to take the best advantage. These structures are used to maximize stiffness at very low weights. The face sheets should be thick enough to withstand tensile and compressive stress induced by the mechanical loads. The overall structure should have high flexural and shear rigidity to avoid high deflections under heavy loads. The face sheets should have sufficient stiffness to provide higher fundamental frequency. The cores should have sufficient shear modulus to prevent buckling of the sandwich under load.

2.2.2 Environmental Considerations

The face sheets and the core should be highly resistant to degradation, moisture and humidity. As the sandwich panel is exposed to harsh environments in space, it should withstand sudden temperature variations and intermittent heating from the sun. Therefore temperature withstanding capability should be a vital factor for the selection of core and face sheet materials. The emissivity and absorptivity values of the face sheets also determine the quantity of heat rejected to the space by radiation. As one of

the face sheets of the sandwich panel is continuously facing the outer space, the absorptivity value will determine the additional heat load on the panel from the sun apart from the heat load from electronics.

2.3 Failure Modes of Sandwich Structures [6]

Sandwich, despite its high stiffness, should also possess high strength. There are five different modes of failure of sandwich composites when loaded in bending. The structure will fail at the mode that occurs at the lowest load. They are

Yielding or fracture of the tensile face

This type of failure occurs when the normal tensile stresses due to the tensile loading exceeds the yield strength of the face sheet materials. This is shown in Figure 2.3.

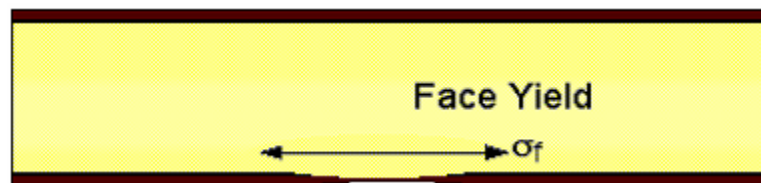


Figure 2.3. Tensile fracture of face sheets of sandwich.

Buckling or Wrinkling of the face

This method of failure occurs due to the excessive compressive stresses, which causes instability in the face sheets. This is shown in Figure 2.4.

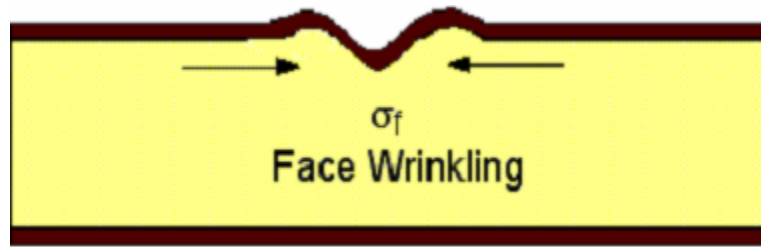


Figure 2.4. Face sheet wrinkling.

Failure of the core in shear

Generally the failure occurs when the shear stress in the core exceeds the shear strength as shown in Figure 2.5. The shear strength of the core depends on the foam density, pore size and the heat treatment temperature.

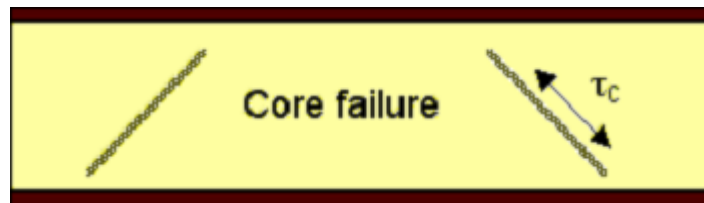


Figure 2.5. Shear failure in the core.

The failure of the bond between the face and the core

This failure occurs only when stresses at the interface (adhesive) are high enough to cause delamination. This is shown in Figure 2.6.

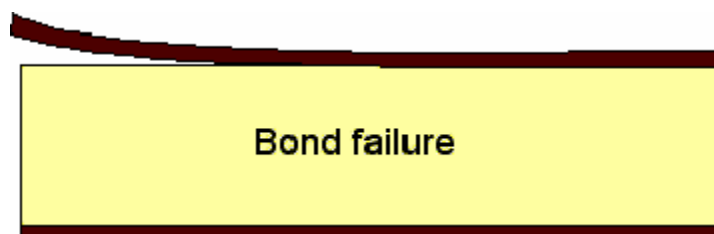


Figure 2.6. Debonding phenomena.

2.4 Stress Distribution in a Sandwich Beam

The stresses in general shear stresses vary parabolically through the thickness of the face and the core. The maximum normal stresses are related to the bending moment M and the distance from the centerline y and the maximum shear stresses are related to the shear force. If the faces are thinner and stiffer than the core, then the stresses can be treated as linear through the thickness of the face sheet and the core. This is shown in Figure 2.7.

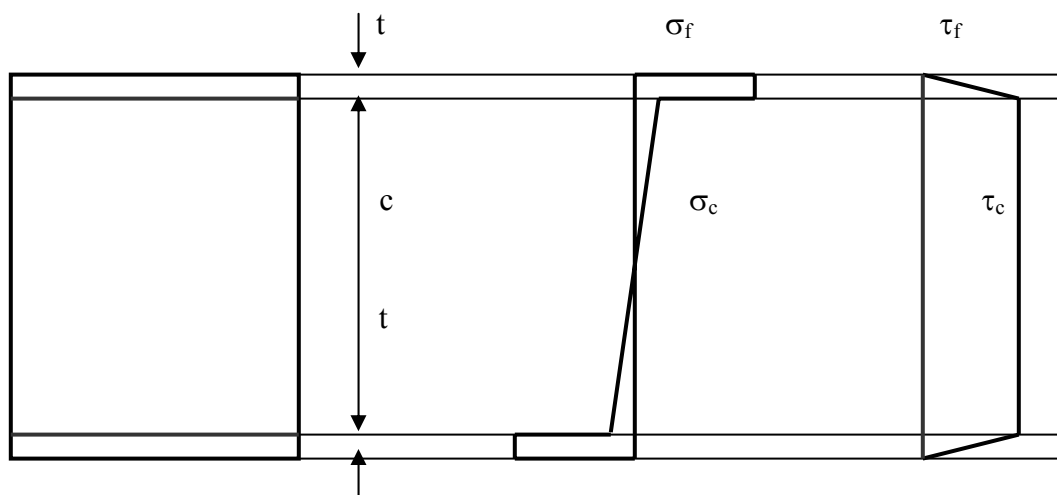


Figure.2.7. Approximate stress distribution in a sandwich beam.

Where, σ_f and σ_c are the normal stresses in the face sheets and the core and τ_f and τ_c are the shear stresses in the face sheets and core.

The mode by which a sandwich structure fails can be established for a given panel geometry and material properties by following the design variables. They are face thickness to span (t/l) and relative density of the core ratios (ρ_c/ρ_f). It is found that face yield is a dominant fracture mechanism at high core densities and face wrinkling is the dominant failure mode at low core densities.

2.5 Literature Review

Several researchers have put forth their models and contributed towards the development of sandwich panels for structural purposes. GLAST LAT (Large Area Telescope) technical document [1] describes the structural design and vibration analysis of all-aluminum radiator panel. A baseline design with a minimum natural frequency and weight budget is provided and the optimum model is chosen. Alternate design options to increase the stiffness of the panel are also considered.

Teti [2] has shown that carbon/carbon radiator panel with aluminum honeycomb core is a good combination of materials for sandwich structures to remove heat from the electronics and also act as a supporting structural member for the EO-1 spacecraft. A thermal balance test, technology validation test (ground test verification) and on-orbit test validation is performed and the results are presented. The pre-flight / experimental and flight analysis data for thermal conductivity is promising and is close to the reported value from the thermal model. The attempt to implement carbon /carbon radiator panel (CCRP) was a success and showed that the technology should be used extensively to solve high temperature thermal management applications.

Klett et al. [9] recently produced the high thermal conductivity graphite foams that can be utilized to provide thermal management solutions to existing problems in spacecrafts and automobiles. It is clearly demonstrated that for weight sensitive thermal management applications or applications where transient conditions often occur, the graphitic foam can be superior in thermal properties to other existing materials. The various potential applications of graphitic foams such as heat sinks and heat exchangers are also discussed. It is also shown that computer chip heat sinks made of graphitic foam had a lesser equilibrium temperature and much lesser weight than that of the same set up with aluminum. It should be noted that specific thermal conductivity of graphitic foams is 6 times higher than that of copper.

Considerable amount of research has been focused on the modeling of sandwich structures and their free vibration response [10-13]. Many of the models proposed to date are based on three dimensional elasticity theory with approximations for the displacements, strains and or stresses through the thickness. These approximations reduce the problem from three-dimensional to two-dimensional one. Depending on the span to depth ratio, panels are referred to as beams (ratio greater than 10) or plates (ratio lesser than 10).

Kant and Swaminathan [14] developed analytical formulations and solutions to the natural frequency analysis of simply supported composite and sandwich plates. It should be noted that Classical Laminate Plate Theory (CLPT) neglects the effect of out of plane strains. As the CLPT under predicts deformations and over predicts natural frequencies and buckling loads, developed higher order shear deformation theories are utilized to take into account the transverse shear and normal deformations for the displacement field.

Kant et al. [15] proposed a complete set of variationally consistent equilibrium equations for the flexure of laminated composite plates and introduced the higher order flexure theory into the finite element formulation. This theory is based on three-dimensional Hooke's law and implements transverse normal and shear deformations.

Reddy [16] developed a set of variationally consistent equilibrium equations for laminated composite plates. Reddy et al. [18] carried out free vibration analysis of isotropic, orthotropic and laminated plates. For laminated plates the results of his theory are found to be in close agreement to three-dimensional elasticity solutions.

Ochoa et al. [18] have studied the effects of geometry, aspect ratio, boundary conditions, and stacking sequence on the free vibrations of laminated composite plates. The study ranges from thin to moderately thick laminates. The laminates are modeled using quadrilateral finite elements that take into account the transverse shear and normal

deformations for through the thickness effects. They also talk about the effects of orientation of the fibers on fundamental frequency for both symmetric and anti-symmetric laminate.

Ochoa et al. [19] conducted an experimental and analytical study of composite panels with multiple cutouts. The response of composites with multiple cutouts is examined under tensile loading. The parameters that govern the stress distribution are the stacking sequence, cutout diameter and cutout geometry. The parametric study provides the user the required knowledge to design optimum cutout geometry based on the mechanical requirements for a laminate. As the radiator panel has a central cutout, the conclusion, that the optimum cutout geometry would be a square and the identification of the localized high stresses due to cutout, is helpful in predicting the stresses.

Swann [20] calculated the maximum temperature difference and the thermal stresses, between face sheets of the sandwich panel. A time dependent prescribed linear temperature source is placed at one side of the face and the other face is insulated. As the core consists of air spaces, not only conduction, but also radiation is incorporated in the heat balance equation. The result is a non-linear partial differential equation with variable coefficients. Assuming that the temperature at the faces of the sandwich is uniform, non-linear partial differential equations are reduced to non-linear ordinary differential equations.

In conclusion, it can be stated that with regard to structural requirements any composite face sheets with a carbon, graphite or an aluminum honeycomb core will exceed the minimum vibration requirement and can sustain the static, dynamic loads developed during launch. Unfortunately, these panels, which are structurally efficient, may not satisfy the thermal requirements for the spacecraft. As the thermal conductivity of the core plays a vital role in dissipating the heat, the selection of the core is very important. Any combination of carbon epoxy composite face sheets with a high thermal

conductivity graphite foam core will be an optimum combination in the aspect of structural and thermal performance for the given thermal management application.

CHAPTER III

FINITE ELEMENT MODELING OF SANDWICH PANEL

The orthotropic nature of each layer of sandwich laminate is represented in MSC Nastran so that stacking sequence and material properties of the radiator panel can be properly incorporated into the analysis. The methodology is discussed in the following sections.

3.1 Material Definition

MSC Nastran supports composite material modeling through the following types of materials. They are

- Orthotropic 2D and 3D
- Anisotropic 2D and 3D

Orthotropic 2D and anisotropic 2D material representations are available for plate elements of triangular and quadrilateral family with linear and parabolic shape functions. The orthotropic 2D and anisotropic 2D material definition utilized in MSC Nastran is presented in Figures 3.1 and 3.2. For orthotropic 3D, there is an additional direction (thickness) for which the material properties must be provided.

It must be noted that 2D, 3D orthotropic and 2D anisotropic material representations do not support steady state and transient heat transfer analysis in MSC Nastran. As one of the foremost requirements is to study the heat transfer abilities of radiator panel, the above mentioned material types cannot be used to represent the finite element model of the panel. Therefore anisotropic 3D material type is implemented for this analysis. However orthotropic 2D material type is implemented for the parametric analysis of free vibration of plates and sandwiches. It should be noted that MSC Nastran needs a

complete elastic matrix for anisotropic materials and separate modulus in 1 (reinforcement) and 2 (transverse) directions for the orthotropic materials.

Figure 3.1. Orthotropic 2D material definition.

Figure 3.2. Anisotropic 2D material definition.

On the other hand solid elements utilize orthotropic 3D and anisotropic 3D material type. The shape of the elements can be four to ten-noded tetrahedron, six to fifteen-noded wedge and eight to twenty-noded brick (hexahedron). Since Orthotropic 3D material does not support heat transfer, anisotropic 3D material type is used to model the composite sandwich panel in the present study. Figures 3.3 and 3.4 shows the material representation for orthotropic 3D and anisotropic 3D definition. The orthotropic 3D material form, in extension to orthotropic 2D, requires properties in three directions fiber, matrix and out of plane. But anisotropic 3D material needs an elastic matrix with 21 constants. The MAT 9 (Refer Appendix 1) entry is used to define an anisotropic material property for all the types of solid elements. Since anisotropic material type is used to define an orthotropic material, it needs nine elastic constants. These constants are calculated using the formulae shown in the appendix.

Define 3D Orthotropic Material			
ID	7	Title	
Color	55	Palette...	
Layer	54	Type...	
Stiffness (E)		Shear (G)	
1	0.	12	0.
2	0.	23	0.
3	0.	13	0.
Poisson Ratio (nu)		Limit Stress	
12	0.	Tension	0.
23	0.	Compression	0.
13	0.	Shear	0.
Expansion (alpha)		Conductivity (k)	
1	0.	0.	0.
2	0.	0.	0.
3	0.	symmetric	0.
Specific Heat, Cp		0.	
Mass Density		0.	
Damping, 2C/Co		0.	
Reference Temp		0.	
Functions >>	ThermoOpt >>		
Phase >>	Nonlinear >>	Load...	Save...
		Copy...	OK
Cancel			

Figure 3.3. Orthotropic 3D material definition.

Figure 3.4. Anisotropic 3D material definition.

3.2 Element Types

The following element types from MSC Nastran are implemented for modeling composites used in radiator panel. They are

3.2.1 2D Laminate Element

It is similar to the plate element, except that this element is composed of one or more layers (lamina). Each layer can represent a different material. MSC Nastran for Windows supports up to 90 layers for a laminate. This element is used to define composite laminate with different thickness and orientation. Figure 3.5 shows Nastran property definition for 2D laminate elements. This element type is used in modeling the sandwich panel for the free vibration response of sandwich panel.

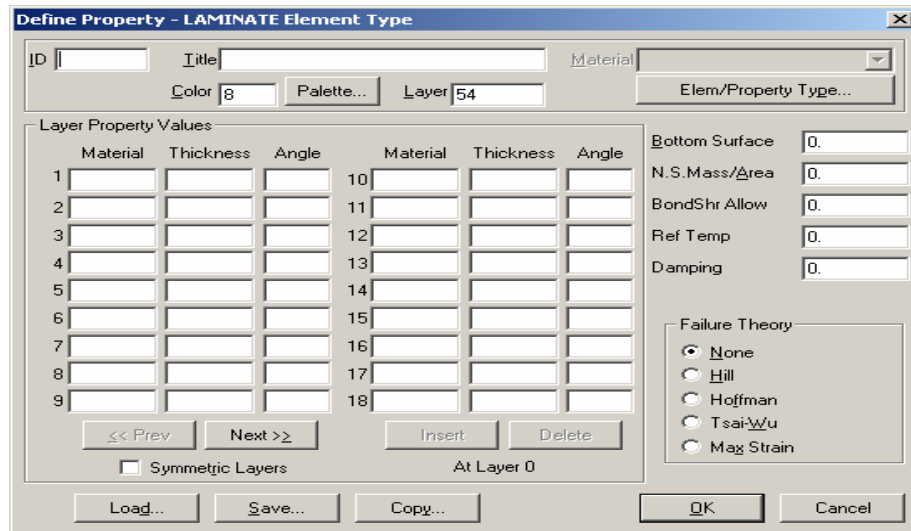


Figure 3.5. 2D laminate type element.

3.2.2 3D Solid Element

It is a volume element type which can be used to model any three dimensional structure. The element type used is three-dimensional eight noded hexahedron. The representation of the 3D eight noded hexahedron element is shown in Figure 3.6. As the material is chosen to be 3D anisotropic with regard to heat transfer analysis, the choice of the element type for all types of analysis needs to be 3D solid elements.

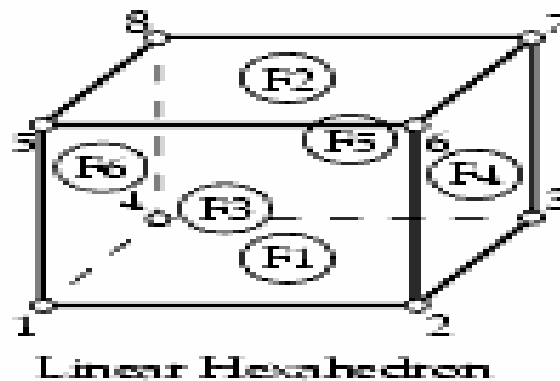


Figure 3.6. Typical eight noded solid element. [21]

3.3 Modeling Classification

The modeling of the sandwich composites has generally fallen into one of the three approaches depending on panel geometry and constituent materials. Accurate prediction of the general or overall instability modes requires adequate representation of the sandwich stiffness. The prediction of the local failures on the sandwich also requires through the thickness modeling. The first type of modeling adopts the standard plate/shell finite elements. This model is referred as layered shell model. The second approach is referred as layered shell/solid model and this incorporates 2 dimensional planar elements for the face sheets and 3 dimensional solid elements for the thick core. This model provides an accurate method for the modeling of sandwich and it depends on through the thickness modeling of the core material. The third approach is a full three-dimensional finite element model that implements three-dimensional solid elements for both the face sheets and the core.

3.3.1 Shell/Shell Representation

This type of model uses the laminate type elements to model the sandwich structure. The sandwich structure with two face sheets and the core is modeled as three groups of layers. The first group of layers represents the composite laminate of the top face sheet. The next set of layers corresponds to middle core material and the final group of layers represents the laminate of the bottom face sheet. The number of groups of layers increases as the number of face sheets increase. This type of modeling usually gives an equivalent single layer approach result using classical laminate theory. The plate elements resist in plane shear and bending forces and can be used for any thin plates and shells. The laminate element type is similar to the plate element except that it is composed of many layers. This representation is implemented in the parametric free vibration analysis of the sandwich panel.

3.3.2 Shell/Solid Representation

Two dimensional plane elements with multi-layers are used to model the face sheets and three-dimensional solid elements are used for the core. One of the demerits of this approach is the displacement field incompatibility between the shell and solid element. Care should be taken in selecting the compatible set of shell and solid elements. Solid elements do not have stiffness in the rotational degrees of freedom at the interface node, which means that only displacements may be transmitted but no moment forces through the interface. One of the methods of handling the transition is to use interpolation elements at the interface. These interpolation elements do not add stiffness to the model but transmit the loading to the adjacent element.

3.3.3 Solid/Solid Representation

This approach does not possess the problem of attaching the solid elements with the plate elements as this model uses three-dimensional solid elements to represent the face sheets and the core. It can be a four to ten noded tetrahedron, six to fifteen noded wedge and eight to twenty noded hexahedron. Therefore solid/solid representation is adopted herein to model the sandwich radiator panel. The face sheets and the core are models generated with solid elements.

3.3.4 Defining the Layers and Stacking Sequence

The most important characteristic of a composite material is its layered configuration. Each layer may be made of a different orthotropic material and may have its principal directions oriented differently. For laminated composites, the fiber directions determine layer orientation. Two methods are available to define the layered configuration.

- By specifying individual layer properties in fiber and matrix directions.
- By defining constitutive matrices that relate generalized forces and moments to generalized strains and curvatures (available only for specific solid elements).

As MAT9 [Refer Appendix 1] entry, which is representing the anisotropic 3D material type, requires a 6 x 6 symmetric material matrix, the composite face sheet is modeled by providing the constitutive matrix. The matrix elements are calculated for each layer separately. The main advantages of the matrix approach are

- It allows an aggregate composite material behavior.
- A thermal load vector may be supplied.
- The matrices may represent an unlimited number of layers.

In the sandwich radiator panel the face sheets are of type T300/5208 carbon epoxy material. The lay-up of the face sheets is chosen to be 0/90 on one side of the core and 90/0 on the other side of the core. The lay-up is said to be symmetric. The face sheets are of composite type with directional material properties. As discussed earlier the face sheets are modeled as a three dimensional anisotropic material using MSC Nastran for windows.

3.4 Material Properties

3.4.1 Face Sheet

The elastic properties for T300/ 5208 carbon epoxy composite are obtained from public database [22].

Elastic Properties [Subscripts 1 – Reinforcement direction, 2 – Transverse direction]

$E_{11} = 181 \text{ Gpa}$, $E_{22} = 10.27 \text{ Gpa}$, $G_{12} = G_{13} = 7.17 \text{ Gpa}$, $\nu_{12} = 0.28$ and $\rho = 1.61 \text{ g/cc}$.

From the expression, $\nu_{12} / E_2 = \nu_{21} / E_1$, ν_{21} is calculated to be **0.016**. From the expression, $G_{23} = E_{22} / 2(1+\nu_{23})$, G_{23} is found to be 3.64 Gpa.

As the material input is in 3D anisotropic form, it is necessary to provide the properties of the composite in the through the thickness direction also. For any composite the thickness properties are difficult to obtain. Therefore it is customarily assumed that the matrix properties apply in the thickness direction. Therefore it can be said,

$$E_{22} = E_{33}, \quad \nu_{12} = \nu_{13}, \quad \text{and} \quad \nu_{21} = \nu_{31}$$

The Poisson's ratio ν_{23} for T300/5208 carbon epoxy composites is **0.42** [23].

$$\nu_{23} = \nu_{32} = \mathbf{0.42}$$

Thermal Properties

Coefficient of Thermal Expansion

$$a_{11} = 0.018 \text{E-06} / ^\circ\text{C}, \quad a_{22} = 22.5 \text{ E-06} / ^\circ\text{C} \quad \text{and} \quad a_{33} = 22.5 \text{ E-06} / ^\circ\text{C}$$

Specific Heat Capacity [24]

$$C_p = 0.94 \text{ J/g-}^\circ\text{K}$$

Thermal Conductivity [24]

$$k_{11} = 2.069 \text{ W/m-}^\circ\text{K}, \quad k_{22} = 0.413 \text{ W/m-}^\circ\text{K} \quad \text{and} \quad k_{33} = 0.413 \text{ W/m-}^\circ\text{K}$$

XX	YY	ZZ	XY	YZ	ZX
26650000.	717800.	717800.	0.	0.	0.
	1810000.	753700.	0.	0.	0.
		1810000.	0.	0.	0.
			1040000.	0.	0.
	symmetric			528400.	0.
					1040000.

Coefficient of Thermal Expansion (A)					
1.E-8	1.25E-5	1.25E-5	0.	0.	0.

Thermal Conductivity (k)					
2.77E-5	5.54E-6	5.54E-6	0.	0.	0.

Spec Ht: 86.94 Mass Density: 0.00015528 Damping: 0. Ref Temp: 450.

Figure 3.7. Material data form of face sheet T300/5208 carbon epoxy. [0]

The material property data form for [0] lamina of T300/5208 carbon epoxy is shown in Figure 3.7. For the [90] lamina of the same material, the material data interchanges based on the orientation of the fibers. It is necessary to create a separate material type for the [90] lamina, due to modeling intricacies in MSC Nastran.

3.4.2 Core

The main focus of the research is to identify and use a core that has high thermal conductivity and low weight. With regard to high conductivity, Poco foam and Poco foam HTC are two of the potential choices for the core. Aluminum honeycomb, with its high stiffness and very low density, also makes a suitable choice as the core of the sandwich radiator panel. All the three core materials are presented in the following discussion. It is to be noted that Poco foam and Poco foam HTC possess isotropic elastic properties but directional thermal properties. The thermal conductivity in the out of plane direction is different from that of the in plane and it is significantly high. Therefore the graphite foam is treated as a 3D anisotropic material in MSC Nastran.

Poco Graphite foam [3]

Elastic Properties

$$E_{11} = E_{22} = E_{33} = 0.40 \text{ Gpa}, G_{12} = 0.14 \text{ Gpa}, \nu_{12} = 0.4 \text{ and } \rho = 0.55 \text{ g/cm}^3.$$

Thermal Properties

Coefficient of Thermal Expansion

$$a_{11} = 0.6\text{E-}06 / ^\circ\text{C}, a_{22} = 0.6\text{E-}06 / ^\circ\text{C} \text{ and } a_{33} = -0.7\text{E-}06 / ^\circ\text{C}$$

Specific Heat Capacity

$$C_p = 0.7 \text{ J/g-}^\circ\text{K}$$

Thermal Conductivity

$$k_{11} = k_{22} = 45 \text{ W/m-}^\circ\text{K} \text{ and } k_{33} = 135 \text{ W/m-}^\circ\text{K}$$

Poco foam HTC has the same elastic properties as that of the Poco foam but different thermal properties. However its density is 0.9 g/cm^3 . It is given as follows.

Thermal Properties

Coefficient of Thermal Expansion

$$a_{11} = 1.03 \text{ E-}06 / ^\circ\text{C}, a_{22} = 1.03 \text{ E-}06 / ^\circ\text{C} \text{ and } a_{33} = -1.09 \text{ E-}06 / ^\circ\text{C}$$

Specific Heat Capacity

$$C_p = 0.7 \text{ J/g-}^\circ\text{K}$$

Thermal Conductivity

$$k_{11} = k_{22} = 70 \text{ W/m-}^\circ\text{K} \text{ and } k_{33} = 245 \text{ W/m-}^\circ\text{K}$$

Aluminum Honeycomb is lightweight and structurally stiff but does not have as high a thermal conductivity as Poco products.

Elastic Properties [25] [Refer Appendix 3]

$E_L = 0.31$ Gpa, $E_W = 0.26$ Gpa and $E_Z = 1.39$ Gpa, $G_{12} = G_{13} = 0.1$ Gpa, $G_{23} = 0.40$ Gpa, $\nu_{12} = 0.33$ and $\rho = 3.68E-02$ g/cm³.

Thermal Properties

Coefficient of Thermal Expansion [26]

$a_{11} = 23.76$ E-06 / °C, $a_{22} = 23.76$ E-06 / °C and $a_{33} = 23.76$ E-06 / °C

Specific Heat Capacity

$C_p = 0.92$ J/g-°K

Thermal Conductivity [Refer Appendix 3]

$k_{11} = 0.67$ W/m-°K, $k_{22} = 1$ W/m-°K and $k_{33} = 1.84$ W/m-°K

The Table 3.1 below summarizes the properties of all the core materials that will be used in MSC Nastran models. It should also be noted that the values shown in the table is compatible with the MSC Nastran system of unit requirements.

Table 3.1

Material properties of sandwich cores.

Classification	Property	Nastran Units	Poco foam	Poco foam HTC	Aluminum honeycomb
Elastic Properties	Young's Modulus				
	E ₁₁	PSI	5.8E04	5.8E04	3.77E04
	E ₂₂	PSI	5.8E04	5.8E04	4.52E04
	E ₃₃	PSI	5.8E04	5.8E04	2.01E05
	Shear Modulus				
	G ₁₂	PSI	20720	20720	15000
	G ₂₃	PSI	20720	20720	58000
	G ₁₃	PSI	20720	20720	15000
	Poisson's ratio ν		0.4	0.4	0.33
Thermal Properties	Expansion Coefficient				
	a ₁₁	in/in-R	3.4E-07	5.7E-07	1.32E-05
	a ₂₂	in/in-R	3.4E-07	5.7E-07	1.32E-05
	a ₃₃	in/in-R	-3.9E-07	-5.9E-07	1.32E-05

Table 3.1 Continued

Thermal Conductivity					
	k_{11}	BTU/in- sec-R	0.0006	0.0009 4	8.8E-06
	k_{22}	BTU/in- sec-R	0.0006	0.0009 4	1.32E-05
	k_{33}	BTU/in- sec-R	0.0018	0.0033	2.42E-05
	Specific Heat Capacity (C_p)	BTU/lb _m -R	65.69	65.69	85.01
Mass Properties	Density (ρ)	lb _m - sec ² /inch 4	5.1E-05	8.4E- 05	3.45E-06

3.5 Sandwich Panel Model

Both the face sheets and the core are modeled as 3D anisotropic material. The sandwich mesh is built in such a way that the nodes at the interface of core and face sheets match against one another and they are merged together as a single node. A corner of the sandwich panel through the thickness is shown in Figure 3.8. The top layer represents the [0] composite face sheet with T300/5208 carbon epoxy properties followed by the [90] face sheet of the same material. The core is represented with two elements through the thickness, as it is thick compared to the face sheets that are made of a single element.

Core elements will represent one of the three above-mentioned materials. The lay-up is symmetric on the other side.

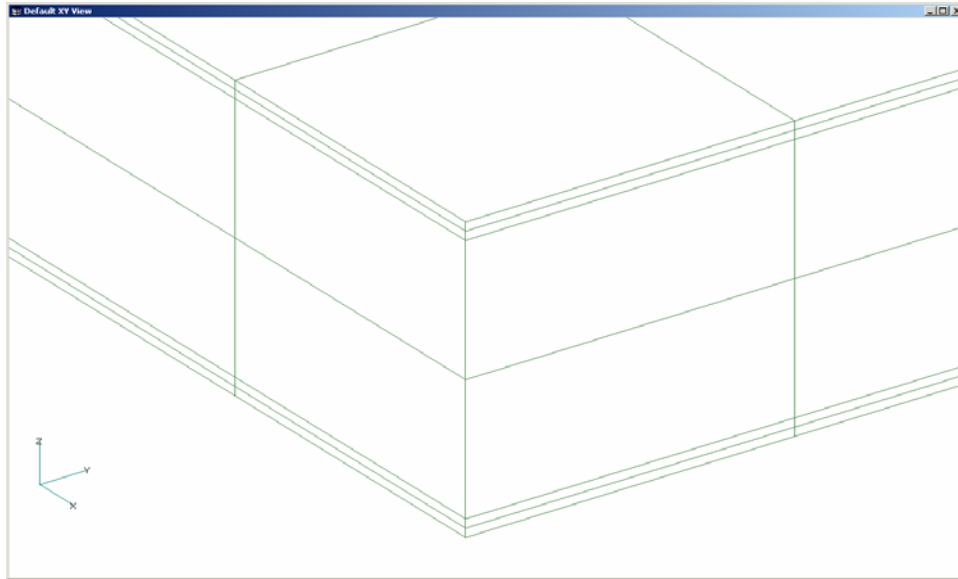


Figure 3.8. Sandwich panel model with face sheets and core. (MSC Nastran)

3.5.1 Cutout

A cutout can be viewed as a boundary having a free edge with localized stress concentration. The model has a rectangle cutout in the middle to hold the antenna. The dimensions of the cut out is 7 x 9 inches with 7 parallel to the longer edge (46 inches) and 9 parallel to the shorter edge (34 inches)

3.5.2 Antenna

The antenna has no physical significance other than its mass contributing to the total weight of the panel. Therefore the mass of the antenna is attached as a nodal mass at the center and it is connected to the inner sides of the cutout using rigid elements. As rigid elements are ignored in heat transfer problems, they do not affect the analysis results.

Rigid element is a rigid link between one independent node and several dependent nodes with respect to certain degrees of freedom. Each of the rigid elements generates internal constraint equations or multi point constraints in MSC Nastran. The constraint equation is used to describe the motion of one dependent degree of freedom in a model as a linear combination of one or more other independent degrees of freedom. The independent degrees of freedom are specified at a single node and the dependent degrees of freedom are specified at an arbitrary number of nodes. The motion at a reference node is defined as a weighted average of the motions at a set of other nodes. The rigid elements are used to model connections that are stiff relative to the remainder of the structure in order to prevent numerical difficulties and often to simplify the model.

3.6 Preliminary Design

The space radiator panel is a sandwich material with **T300/5208 carbon/epoxy** face sheets and a foam and aluminum honeycomb core. The lay-up of the sandwich Panel is **0/90/core/90/0**. The thickness of the core is assumed to be 0.6 inch and the thickness of each face sheet is 0.02 inch. Its overall dimensions are as follows, panel 46X34 inches, center cutout 7X9 inches.

The space radiator sandwich panel design constraints are fundamental frequency of more than **100Hz** with the boundary edges fixed in all the degrees of freedom, dissipate heat flux of **100 W/m²**, withstand static loads of 10G and dynamic launch loads acting during each stage of spacecraft. The Figure 3.9 below shows the complete sandwich panel modeled with 3D elements with the antenna modeled as mass and rigid elements at the cutout.

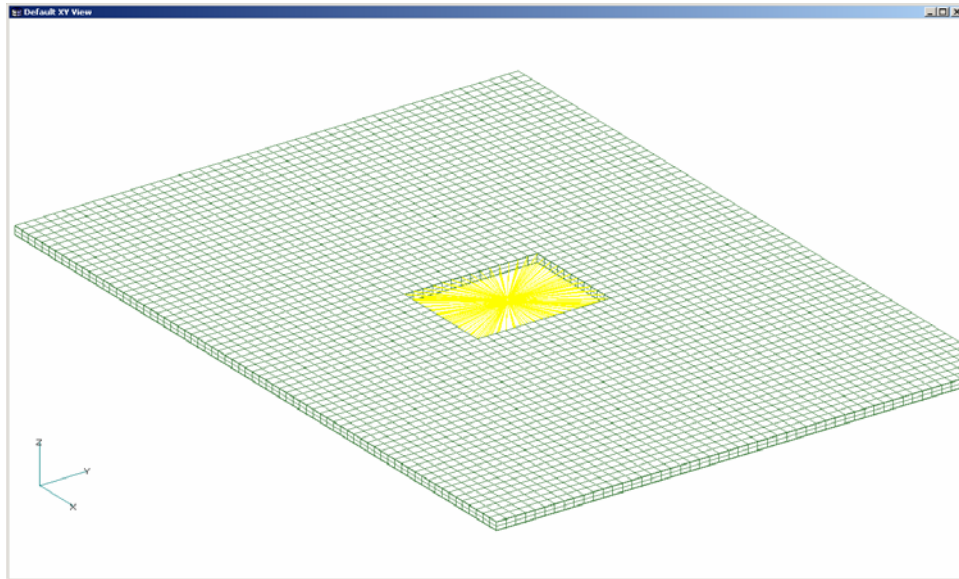


Figure 3.9. Sandwich radiator panel with antenna at the cutout.

CHAPTER IV

VIBRATION AND THERMAL CHARACTERISTICS OF SANDWICH RADIATOR PANEL

4.1 Plate Theory

The assumptions inherent in the analysis of a composite sandwich radiator panel in this effort are

- body forces neglected
- mid-plane symmetric
- no hygrothermal effects,
- without shear coupling terms and
- subjected to a lateral load $p(x, y)$

Then the equilibrium equations can be expressed as

$$\frac{\partial M_x}{\partial x} + \frac{\partial M_{xy}}{\partial y} - Q_x = 0 \quad (4.1)$$

$$\frac{\partial M_{xy}}{\partial x} + \frac{\partial M_y}{\partial y} - Q_y = 0 \quad (4.2)$$

$$\frac{\partial Q_x}{\partial x} + \frac{\partial Q_y}{\partial y} + p(x, y) = 0 \quad (4.3)$$

After simplifying and neglecting the transverse shear deformation for preliminary design stage these equations result in the following governing differential equation for a sandwich plate subjected to bending.

$$D_{11} \frac{\partial^4 w}{\partial x^4} + 2(D_{12} + 2D_{66}) \frac{\partial^4 w}{\partial x^2 \partial y^2} + D_{22} \frac{\partial^4 w}{\partial y^4} = p(x, y) \quad (4.4)$$

In real life, many structures and products are subjected to dynamic loads. These dynamic effects may be due to natural vibrations or forced vibrations. As this problem focuses on the free vibration effects, it is of practical significance to discuss the natural vibration characteristics of composite plates and sandwiches. It is known that each structure has infinite natural frequencies and only a few of which are important such as the fundamental mode. At this frequency the structure may exceed the yield strength and its behavior changes drastically. Mathematically, these frequencies are non-trivial solutions called “Eigen” values of the homogeneous equations and the corresponding “Eigen” vector determines the mode shape of the structure. This study of natural frequency becomes more important when a forcing function excites the structure at its fundamental frequency. The largest amplitude of response will be in the mode shape whose natural frequency is closest to that of the forcing function. The source of vibration in a spacecraft is from the dynamic loads acting during various stages such as launch and descent. As the radiator sandwich panel is bound to experience such loads, it is necessary to determine its natural frequency. Therefore in the following sections, the natural frequency calculation of composite plates and sandwiches are presented.

4.2 Free Vibration of a Simply Supported Rectangular Plate

The governing differential equation for free vibration without in plane or lateral forces and subjected to dynamic loading [28] is given by

$$D_{11} \frac{\partial^4 w}{\partial x^4} + 2(D_{12} + 2D_{66}) \frac{\partial^4 w}{\partial x^2 \partial y^2} + D_{22} \frac{\partial^4 w}{\partial y^4} + \rho \frac{\partial^2 w}{\partial t^2} = 0 \quad (4.5)$$

Converting the dynamic problem to a static problem by applying D'Alemberts principle and applying the boundary conditions for simply supported case,

$$x=0, a \quad w(x, y) = 0 \text{ and } M_x = 0$$

$$y=0, b \quad w(x, y) = 0 \text{ and } M_y = 0$$

we get

$$\omega_{mn}^2 = \frac{\pi^4}{b^4 \rho} \left[D_{11} \left(\frac{mb}{a} \right)^4 + 2(D_{12} + 2D_{66}) \left(\frac{nmb}{a} \right)^2 + D_{22} n^2 \right] \quad (4.6)$$

The lowest or the fundamental frequency is obtained by substituting $m=n=1$

$$\omega_{11} = \frac{\pi^2}{b^2 \sqrt{\rho}} \sqrt{\left[D_{11} \left(\frac{b}{a} \right)^4 + 2(D_{12} + 2D_{66}) \left(\frac{b}{a} \right)^2 + D_{22} \right]} \quad (4.7)$$

For an isotropic plate $D_{11} = D_{12} = D_{66} = D_{22} = D$. Therefore the fundamental frequency is given by

$$\omega_{11} = \frac{\pi^2 \sqrt{D}}{b^2 \sqrt{\rho}} \sqrt{\left[\left(\frac{b}{a} \right)^4 + 2 \left(\frac{b}{a} \right)^2 + 1 \right]} \quad (4.8)$$

Where,

a and b – length and width of the rectangular plate

ρ - Density of the material of the plate

$w(x, y)$ – displacement function of the plate

M_x, M_y – Moments about x and y-axis.

D – Flexural stiffness of the isotropic plate

D_{xy} – components of flexural stiffness modulus if the plate is orthotropic.

4.3 Parametric Study of Simply Supported Plates and Sandwiches.

A simple parametric study of the fundamental frequency of isotropic, orthotropic, laminated and sandwich plates is undertaken. The dimensions of the plate are assumed to be the same as the radiator panel. The variations of the fundamental frequency are shown as a function of the thickness of the plates for different material types. In the case of orthotropic plates, it is shown as a function of the orientation of the fibers. These results are also supported with corresponding finite element models in MSC Nastran. The results of closed form model are in good agreement with finite element solution. The error percent is less than 2. It should be noted that 2D plate elements with orthotropic material properties are used to model the plates in MSC Nastran. In this analysis the following assumptions are made as part of solving the given problem. The assumptions are

- The plate aspect ratio (a/h) is 80-100 where “a” is the length of the Plate and “h” is the thickness of the plate.
- there are no transverse shear deformations (e_{xz})
- it is mid-plane symmetric.
- there are no shear coupling terms.
- there are no applied surface and in-plane forces
- there are no hygrothermal effects
- all the edges of the plate are simply supported.

4.3.1 Aluminum 2024-T3 Isotropic Plate

Plate Dimensions: All units are in English system.

$a = 46$ inches, $b = 34$ inches, $h = 0.51$ inches, Aspect ratio (a/h)=90.20

Material Properties:

Young's Modulus (E) = 1.06E07 Psi

Mass Density (Weight Density/Gravity)(ρ_m) = 0.000258 lb-sec²/inch⁴

Poisson's Ratio (ν) = 0.3

The fundamental frequency of an isotropic plate in radians per unit time is given by

$$\omega_{11} = \frac{\pi^2 \sqrt{D}}{b^2 \sqrt{\rho}} \left[\left(\frac{b}{a} \right)^2 + 1 \right] \text{ rad/sec or } F_n = \omega_{11} / 2\pi \quad (4.9)$$

Where $D = E \cdot h^3 / (12 \cdot (1 - \nu^2))$

The fundamental frequency (F_n) is found to be **65.65Hz**. The variation of the frequency with the thickness of the plate is shown in Figure 4.1.

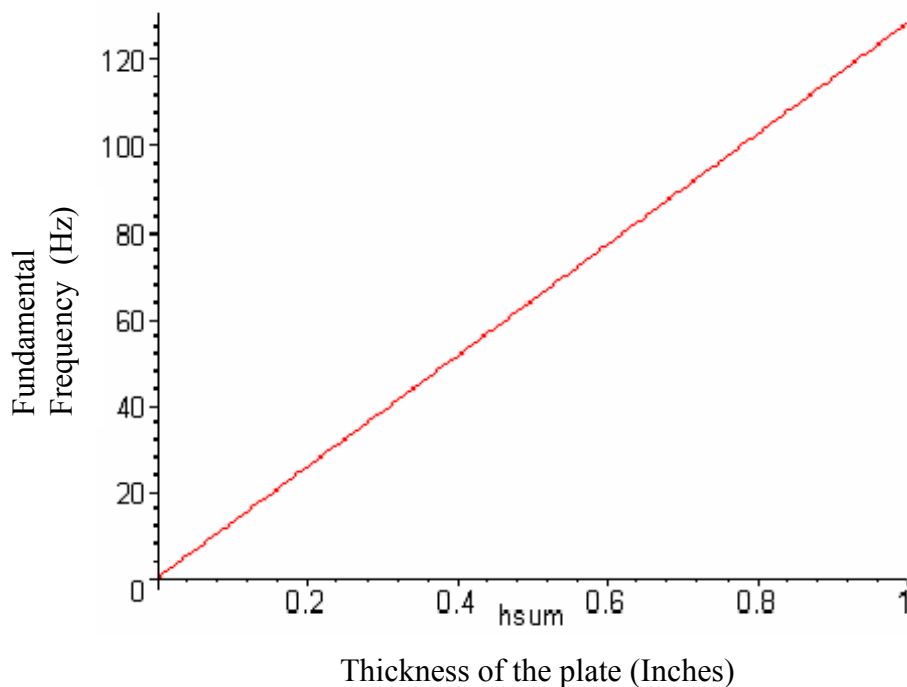


Figure 4.1. The variation of the fundamental frequency with the thickness of the isotropic plate.

4.3.2 T300/5208 Carbon/Epoxy Composite Plate

Lay-ups

Multi-layered specially orthotropic plate 0/90/90/0 or [0/90]_s scenario is considered.

Material Properties

$$E_{11} = 21\text{E}6 \text{ psi}$$

$$E_{22} = 1.76\text{E}6 \text{ psi}$$

$$G_{12} = 0.65\text{E}6 \text{ psi}$$

$$\nu_{12} = 0.21$$

$$\nu_{21} = 0.0176$$

$$\rho_m = 0.000155 \text{ lb. -sec}^2/\text{inch}^4$$

The fundamental frequency of a specially orthotropic plate [33] is given by the following

$$\omega_{11} = \frac{\pi^2}{b^2 \sqrt{\rho}} \sqrt{\left[D_{11} \left(\frac{b}{a} \right)^4 + 2(D_{12} + 2D_{66}) \left(\frac{b}{a} \right)^2 + D_{22} \right]} \quad (4.10)$$

Where $D_{ij} = \frac{1}{3} \sum_{k=1}^N \bar{Q} \left(\frac{h_i(k)}{2} \right)^3$ and N is the number of layers

and

$$Q_{matrix} = \begin{bmatrix} \frac{E_{11}}{1-\nu_{12}\nu_{21}} & \frac{\nu_{21}E_{11}}{1-\nu_{12}\nu_{21}} & 0 \\ \frac{\nu_{12}E_{22}}{1-\nu_{12}\nu_{21}} & \frac{E_{22}}{1-\nu_{12}\nu_{21}} & 0 \\ 0 & 0 & G_{12} \end{bmatrix} \quad (4.11)$$

$$\bar{Q} = \begin{bmatrix} m^2 & n^2 & 2mn \\ n^2 & m^2 & -2mn \\ -mn & mn & m^2 - n^2 \end{bmatrix} \begin{bmatrix} \frac{E_{11}}{1-\nu_{12}\nu_{21}} & \frac{\nu_{21}E_{11}}{1-\nu_{12}\nu_{21}} & 0 \\ \frac{\nu_{12}E_{22}}{1-\nu_{12}\nu_{21}} & \frac{E_{22}}{1-\nu_{12}\nu_{21}} & 0 \\ 0 & 0 & G_{12} \end{bmatrix} \begin{bmatrix} m^2 & n^2 & 2mn \\ n^2 & m^2 & -2mn \\ -mn & mn & m^2 - n^2 \end{bmatrix} \quad (4.12)$$

Where $m = \cos(\theta)$ and $n = \sin(\theta)$

The fundamental frequency value for the lay-up is found to be

$$\mathbf{0/90/90/0} \quad \omega_{11} = \mathbf{343.48} \quad F_n = \mathbf{54.64}$$

4.3.3 Sandwich Plate with Two Identical Face Sheets of T300/5208 Carbon/Epoxy and a Foam Core

Lay-up considered: [0/90/core/90/0]

Face Sheet Properties

$$E_{11} = 21E7 \text{ psi}$$

$$E_{22} = 1.76E7 \text{ psi}$$

$$G_{12} = 0.65E7 \text{ psi}$$

$$\nu_{12} = 0.21$$

$$\nu_{21} = 0.0176$$

$$\rho_m = 0.000155 \text{ lb-sec}^2/\text{inch}^4$$

$$t_f (\text{Thickness of each face sheet}) = 0.005 \text{ inch}$$

Core Properties

$$E_c = 1.7E7 \text{ psi}$$

$$G_c = 10000 \text{ psi}$$

$$\nu_c = 0.4$$

$$\rho_m = 2.24638E-6 \text{ lb-sec}^2/\text{inch}^4$$

$$h_c (\text{Thickness of the core}) = 0.5 \text{ inch}$$

The fundamental frequency of a specially orthotropic plate is given by the equation 4.10.

Where, $D_{ij} = \frac{1}{3} \sum_{k=1}^N \bar{Q} * \left(\frac{h_i(k) - h_i(k-1)}{2} \right)^3$ and N is the number of layers. In this case the value of N is 4

The Non-dimensional frequency is given by

$$\bar{W} = \frac{W_{mn} * b^2}{h_{total}} \left(\frac{\rho}{E_{22}} \right)_f^{0.5} \quad (4.13)$$

The fundamental frequency determined from the calculation is shown in Table 4.1. The variations of the fundamental frequency with the parameters of the sandwich are shown in Figures 4.2, 4.3 and 4.4. The plot provides the fact that the stiffness is directly proportional to the thickness of the core. It is understood that the stiffness increases by keeping the face sheets apart. A non-dimensional parameter (h_c / t_f) is plotted against the frequency in figure 4.3. It provides that face sheet stiffnesses are vital in providing the

overall stiffness of the sandwich. Figure 4.4 shows the variation of the fundamental frequency with the individual face sheet thicknesses.

Table 4.1

Non-dimensional fundamental frequency for sandwich plate.

Lay-up	Height of the Core (h_c) in inches	Thickness of the Face Sheet (t_f) in inches		ω_{11} in Radians per unit time	F_n in Hertz	Non-dimensional frequency (\bar{W})
		t_{f1}	t_{f2}			
0/90Core/90/0	0.5	0.005	0.005	1014.381	161.379	21.1815

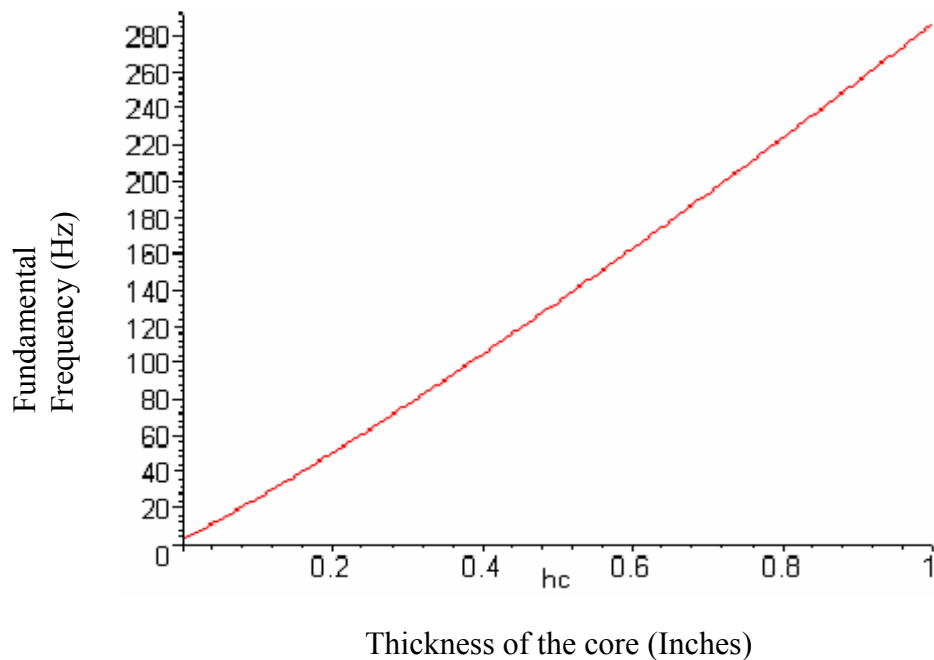


Figure 4.2. The variation of the fundamental frequency with the thickness of the core. (h_c) (keeping the thickness of the face sheet (t_f) as constant)

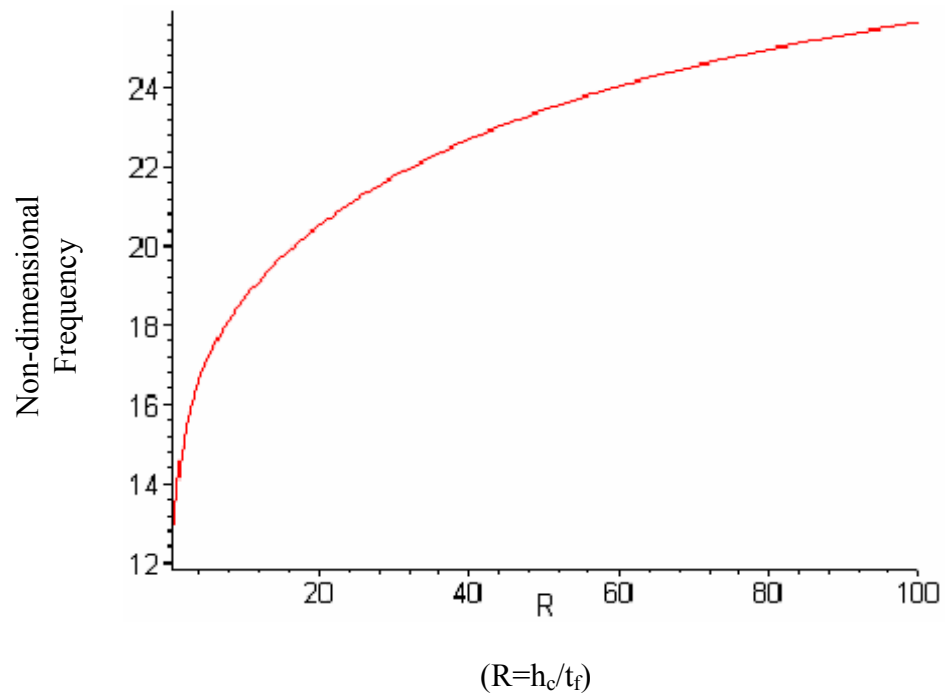


Figure 4.3. The variation of the non-dimensional frequency with the parameter R.

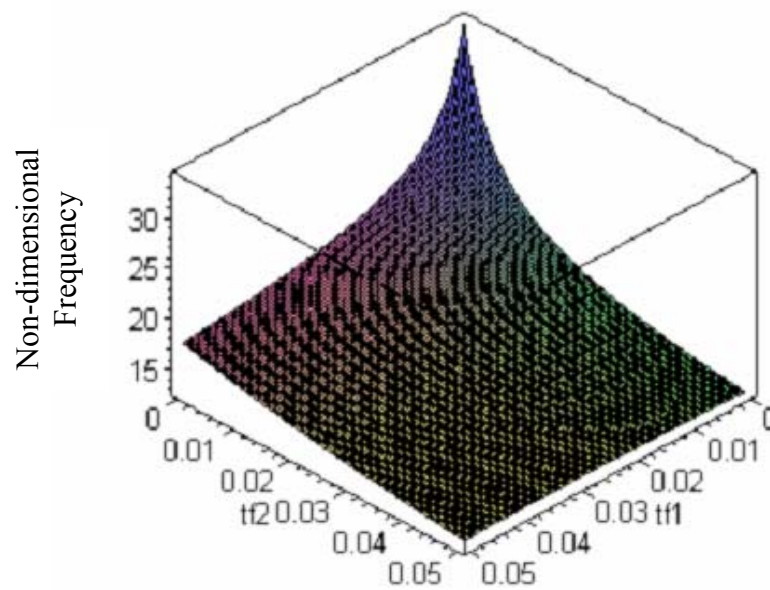


Figure 4.4. The variation of the non-dimensional frequency with the face sheet thicknesses. (t_{f1} and t_{f2}) (core thickness (h_c) is constant)

4.4 Sandwich Panel Design

The closed form solution of section 4.3 illustrates the effect of plate geometry, aspect ratio, support conditions and lamina stacking sequence on the natural frequencies of specially orthotropic fiber reinforced composite plates and sandwiches. Both the material properties and the support conditions are not representative of the radiator design. Herein, the actual materials for the face sheet and the core are incorporated into the analysis. The material of the face sheets is T300/5208 carbon epoxy. The elastic and thermal properties of T300/5208 carbon epoxy [22] composite are shown in Table 4.2.

Table 4.2

Properties of T300/5208 carbon epoxy.

Elastic Properties [22]	Young's Modulus	E_{11}	2.63E07	Psi
		$E_{22}=E_{33}$	1.49E06	Psi
	Shear Modulus	$G_{12}=G_{13}$	1.04E06	Psi
		G_{23}	5.28E05	Psi
	Poisson's Ratio	$\nu_{12}=\nu_{13}$	0.28	
		ν_{23} [23]	0.42	
	Density	ρ	0.00015	$\text{lb}_m\text{-sec}^2/\text{inch}^4$
Thermal Properties	Thermal Conductivity [24]	K_{11}	2.77E-05	Btu/in-sec-R
		$K_{22}=K_{33}$	5.54E-06	Btu/in-sec-R
	Coefficient of Thermal Expansion [22]	A_{11}	1E-08	In/in-R
		$A_{22}=A_{33}$	1.25E-05	In/in-R
	Specific Heat Capacity [24]	C_p	86.94	Btu/ $\text{lb}_m\text{-R}$

The material choices of the core are Poco foam products and aluminum honeycomb. The material properties can be found in Table 3.1

4.4.1 Basic Approach

One of the foremost design criteria for the radiator panel is the natural frequency. It should be above 100 Hz to sustain the vibration during the launch and descent of spacecraft. Aluminum is extensively used as face sheets in sandwich panels, however in the current proposed design, carbon/epoxy layers are used as face sheets. The laminate thickness that satisfies stiffness requirement is also a design variable and needs to be determined. Furthermore additional variables such as stacking sequence, and number of layers are also incorporated in the design. Through parametric studies via finite element analysis, various lay-ups are considered to identify the appropriate one for the radiator panel.

The parametric study of section 4.3 on free vibrations of the sandwich panel suggests that [0/90/core/90/0] lay-up has a fundamental frequency greater than 100 Hz with the given dimensions for the sandwich face sheets and core. This baseline design indicates that [0/90/core/90/0] lay up can be considered as a candidate for the radiator panel. Since [0/90/core/90/0] sandwich lay-up is specially orthotropic and symmetric, it has no bending coupling nor shear and torsion coupling. Therefore for the above-mentioned lay-up, a finite element model is set up in MSC Nastran with the material properties of appropriate face sheets and core of table 4.2 and 3.1. The most efficient sandwich panel response depends on thin face sheets that are separated far enough with a thick core. Increasing the stiffness and thickness of the panel leads to a weight increase thus care should be taken in selecting the density of the core as well as its thickness. It is also necessary to select the material systems that meet the thermal requirements. This demands a rigorous optimization of the sandwich parameters such as core and face sheet thicknesses, lay-up and orientation to satisfy the required design criteria and to bring out

the best lay-up for the radiator panel. Much of optimization for the radiator panel is presented in the chapter on Numerical Results and Discussions.

4.4.2 Support Conditions

For the models, the sandwich radiator panel is fully constrained (displacements and rotations) on all the four edges. Even though, in service environment it is to be mounted with certain spacing of bolts to provide the required stability during launch and descent, an assumption to fully constrain all the edges is made for analysis purposes. The edge constraints influence greatly the natural frequencies and their corresponding mode shapes. The numbers 1 to 6 represents the translation and rotational degrees of freedom. The Nastran model with the support conditions is shown in the Figure 4.5.

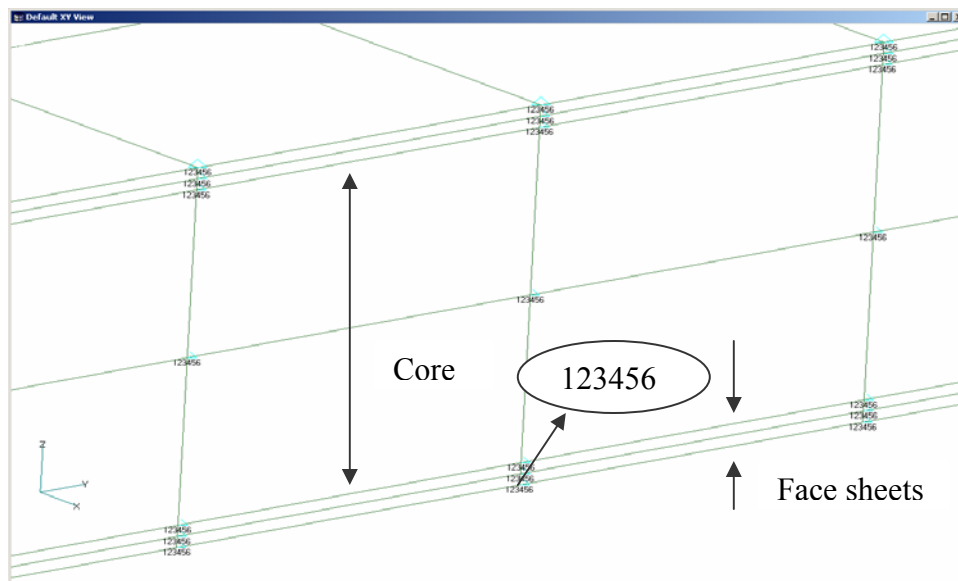


Figure 4.5. Edge constraints of sandwich radiator panel.

Since in the design of radiators, density is an important factor, the Poco foam vs. Poco foam HTC is selected to conduct this study. On the other hand, aluminum honeycomb is less dense than foam but its thermal conductivity is lower.

4.5 Static and Dynamic Characteristics of Radiator Panel

The governing differential equation for the bending of a composite material plate with mid plane symmetry, without bending-twisting coupling and transverse shear deformation (classical plate theory) and subjected to laterally distributed load $p(x, y)$ is as given by equation 4.14.

$$D_{11} \frac{\partial^4 w}{\partial x^4} + 2(D_{12} + 2D_{66}) \frac{\partial^4 w}{\partial x^2 \partial y^2} + D_{22} \frac{\partial^4 w}{\partial y^4} = p(x, y) \quad (4.14)$$

Pagano [29] provides an exact solution to the problem of a rectangular orthotropic sandwich plate subjected to a laterally distributed load.

A general governing equation used in the structural analysis is given in equation 4.15.

$$[M]\{u(t)\} + [B]\{u(t)\} + [K]\{u(t)\} = \{P(t)\} \quad (4.15)$$

The above equation is a general one that includes inertia, damping forces and load can be changed with respect to time. But in static analysis load does not change with respect to time, inertia forces and damping are not considered and therefore the above equation reduces to

$$[K]\{u\} = \{P\} \quad (4.16)$$

where $[K]$: stiffness matrix

$\{u\}$: node displacement vector

$\{P\}$: load vector

The linear static analysis is the most basic type of analysis in which the displacement or stress is directly proportional to load or force applied and it is independent of time. Some examples of static loadings are

- A time invariant dead load (like a building load)
- Enforced displacement and
- Steady state temperature field.

The loadings can be independent or more often combined with each other as multiple loading that reduces the time taken and improves the solution efficiency. Once the displacements are computed, MSC Nastran uses these to compute element forces, stresses, reaction forces and strains.

4.5.1 Static Loading

The sandwich radiator panel with its antenna mass is subjected to a static loading of “10g” in the direction perpendicular to the plane of the panel. The objective of static loading is to define the resulting load distribution throughout the structure. When performing static analysis with load factors, inertial (“g”) forces are applied to the structure. Inertial forces in all three axes can be applied simultaneously including sign combinations. The linear static analysis in MSC Nastran provides the stresses and strains in the sandwich panel. Since the panel dimensions are in inches, the equivalent loading in English system of units is given by

$$\begin{array}{l} 1g \quad = 386.4 \text{ inch/sec}^2 \\ \text{Therefore } 10g \quad = 3864 \text{ inch/sec}^2 \end{array}$$

4.5.2 Dynamic Loading

Payloads and spacecraft are designed to maintain structural integrity and degree of functionality to ensure successful operation during all phases of the expected life cycle. The design of Space flight components in general should consider static and dynamic loads to be encountered during assembly, testing, transportation, launch, ascent, space operations, extraterrestrial operations, descent and landing.

4.5.2.1 Requirements

- **Load Regimes**

For a spacecraft or a payload, there is a need for a thorough understanding of its operation and performance to ensure complete definition of load requirements.

1. During the design process all the load regimes to which the structure is exposed should be evaluated.
2. If the structure has multiple load configurations during its mission, the individual load configurations are identified
3. Within each load regime, each source of loading is identified. Different load sources that can occur simultaneously shall be coupled together.

- **Requirements for payloads**

Evaluation of loads for the payload is an iterative process. First, the preliminary design loads are incorporated for the initial sizing of the structure. Then a mathematical model of the structure is developed and a preliminary load cycle is performed. Based on the resulting load values, the initial structure sizing values need to be adjusted. Subsequent load cycles are needed to assess the changes in design, launch vehicle and payload mathematical models, and forcing functions.

1. **Preliminary Design Loads:** This load data set is used for the initial sizing of structural elements to begin the load analysis process. The structural elements comprises of the primary structure and the components.
2. **Development of mathematical models for loads:** A mathematical model for the payload is developed using finite element methods and it is then coupled with launch vehicle to perform one or more cycles of analysis in order to update the loads in the payload. The model may be a reduced version of the finite element model using static or dynamic reduction methods or a model specifically developed for load analysis. This approach will be aimed at producing accurate dynamic predictions. (Frequencies, mode shapes and stresses)
3. **Forcing Functions:** Forcing functions associated with each event in a launch vehicle are provided by Launch Vehicle Organization and are intended to yield load responses.
4. **Load Cycles:** A minimum of two load cycles, one a preliminary load cycle and the other verification load cycle that uses test-verified models, are performed on the launch vehicle.
5. **Load Combinations:** In many cases the loads produced by different environments can occur simultaneously and these loads can be coupled to define the limit load. In a shuttle the most common types of load combinations are transient loads with random vibration loads due to liftoff and transient loads with thermal loads due to landing.
6. **Verification of the payload mathematical model:** This procedure shall be performed to ensure the safety and accuracy of the model for stress and deflection predictions.

The requirements for spacecraft have similar design parameters to be evaluated as in design of payloads. However the spacecraft configuration may change as deployments and separations occur and the structure may be different.

4.5.2.2 Load Regimes

Typical load regimes for payload and spacecraft are

Lift off and Ascent

This environment may vary depending on the type of launch vehicle used. This may include engine ignition, launch pad release, liftoff, maximum dynamic pressure, maximum acceleration, separations, engine shutdowns and thrust oscillations. The major induced source for the dynamic loading is from the propulsion system operation. Some of the basic types of flight environments that generate dynamic loads on payload are

- Low frequency dynamic response,
- High frequency random vibration environment and
- High frequency acoustic pressure environment

Space Operations

Space Operations may induce mechanical and thermal loads on the structure. Some of the possible sources for mechanical loading are rotating machinery, deployment and robotics activity. Thermally induced loads may result from internal heat sources and radiators.

Descent and Landing

This event is a transient loading environment where payloads and spacecraft will be subjected to static and dynamic loading. Descent maneuvers, landing gear impact, thermal loadings resulting from orbit operations and post-landing loads shall be considered

4.5.3 Designing for Random Vibration

The fundamental nature of random vibration and fatigue must be understood clearly in order to design, develop and produce cost effective and lightweight structures that are capable of operating in various environments with high degree of reliability. The dynamic load path must be examined when it passes through the structure to make sure there is no failure at weak locations. The characteristic of random vibration is non-periodic and it can be considered as a series of overlapping sinusoidal curves. In this environment all the exciting frequencies within a given bandwidth are excited at the same time.

4.5.3.1 Random Vibration Input Curve

One of the different types of curves that can be used to show the random vibration input requirements is the Power Spectral Density (PSD) curve. This is shown in log-log scale with power spectral density (G^2/Hz) along the vertical axis and frequency (Hz) along the horizontal axis. It should be noted that acceleration is represented as root mean square (RMS) and it is the area under the random vibration curve. The figure 4.6 shows the shaped random vibration input curve for the sandwich radiator panel.

Normal and In-plane to mounting Surface (X, Y and Z-axis)

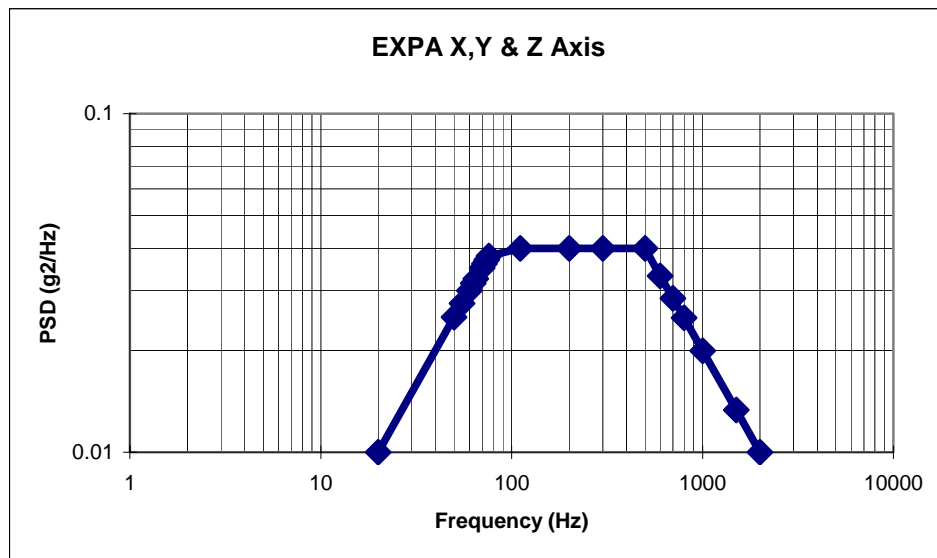


Figure 4.6. Power spectral density levels.

4.5.3.2 Dynamic Load Set Calculation

Once the fundamental frequency of the radiator panel is predicted, the Power Spectral Density value is obtained from the above graph. The estimate of static accelerations due to random vibration loads based on Power Spectral Density (PSD) is called as NRV (Random Vibration) load set. The procedure to calculate these dynamic loads is shown in the Table 4.3. The table is self explanatory in the method of calculation. The load regimes considered for the calculation of random vibration loads are “lift off” and “landing”. The other load regimes such as “on orbit deployment and assembly” and “space operations” are neglected, as they do not contribute to dynamic loads. The inertia load cases for the “lift off” and “landing” are in accordance with Launch Vehicle Organization standards.

Table 4.3

Random vibration load set calculation for radiator panel

NRV load Set Calculation				
Magnification Factor (Q)	Sqrt (F_n)			
Lowest Natural Frequency, (F_n)	First Mode of the panel.			
PSD (X, Y) at F_n	From Fig. 4.7.			
PSD (Z) at F_n	From Fig. 4.7.			
NRV_{xy}=3*sqrt(PI/2*Q*Fn*PSD) (Random Vibration Loads)	Calculated using above values			
NRV_z=3*sqrt (PI/2*Q*Fn*PSD) (Random Vibration Loads)	Calculated using above values			
Inertia Load Cases in G's [Launch Vehicle Organization Standards]	Event	N_x	N_y	N_z
Transient	Lift -off	6.6	4.2	5
	Landing	7.2	5.9	6.3
Quasi-static	Ascent			
	On-orbit			
	Descent			
Load Sets in G's		X Axis	Y Axis	Z Axis
Set 1		N_x+NRV_x	N _y	N _z
Set 2		N _x	N_y+NRV_y	N _z
Set 3		N _x	N _y	N_z+NRV_z

The Table 4.3 provides three sets of random vibration loads in all the three directions. The sandwich radiator panel is subjected to each load set and the stress and deformation characteristics are predicted using MSC Nastran. It is to be noted that fundamental frequency of the panel will vary with the type of core and dynamic loads are based on the lowest mode of the structure as mentioned in the Table 4.3. The following Figure 4.7 shows the load entry form at MSC Nastran. As the values of load sets are required in inch /sec², it is necessary to convert the load set in G's to inch / sec².

The screenshot shows the 'Create Body Loads' dialog box with the following details:

- Load Set 1** (Untitled)
- Acceleration**
 - Active**
 - Translation/Gravity (length/time/time): X: 0., Y: 0., Z: 0.
 - Rotation (radians/time/time): Ax: 0., Ay: 0., Az: 0.
- Velocity**
 - Active**
 - Rotation (rev/time): Wx: 0., Wy: 0., Wz: 0.
- Origin**
 - Active**
 - Center of Rotations: X: 0., Y: 0., Z: 0.
- Thermal**
 - Active**
 - Active**
 - Default Temperature: T: 0.
 - Reference Temperature: RefT: 0.
- Buttons: **OK**, **Cancel**

Figure 4.7. Dynamic load set for radiator panel.

4.6 Heat Transfer Analysis of Radiator Panel

Composite structures after fabrication operate in a variety of thermal environments that may directly impact on performance. These thermal effects are a result of temperature variations and heat flux additions and are directly related to the thermal properties of the constituents. Composite sandwich structures should be carefully analyzed and designed to meet very close thermal tolerances for structures that are critically important like communication satellite antennas, reflectors or any other terrestrial systems.

The thermal state affects the stress-strain behavior of composite materials since the properties of the individual constituents vary with temperature and generate residual stresses. The thermal effects are most noticeable in matrix and less in fibers as they are less sensitive to environment. The thermal behavior of a lamina is characterized by its two principal coefficients of thermal expansion (CTE), α_1 and α_2 . 1 and 2 denote the longitudinal and transverse material coordinate directions. A lamina undergoes thermal deformation when subjected to a change in temperature ΔT . The linear thermal strains in the principal material axes of the lamina are

$$\begin{aligned} e_1 &= \alpha_1 \Delta T \\ e_2 &= \alpha_2 \Delta T \\ e_6 &= 0 \end{aligned} \quad (4.17)$$

These thermal strains can be transformed to global co-ordinates e_x , e_y and e_s by the transformation matrix. When a multidirectional laminate is subjected to mechanical and thermal loading, any k^{th} lamina in the laminate is under a state of stress $[\sigma]_{x,y}^k$ and deformation $[\varepsilon]_{x,y}^k$. The strain relation is given in the equation 4.18.

$$\begin{bmatrix} \varepsilon_x \\ \varepsilon_y \\ \gamma_s \end{bmatrix} = \begin{bmatrix} S_{xx} & S_{xy} & S_{xs} \\ S_{yx} & S_{yy} & S_{ys} \\ S_{sx} & S_{sy} & S_{ss} \end{bmatrix} \begin{bmatrix} \sigma_x \\ \sigma_y \\ \tau_s \end{bmatrix} + \begin{bmatrix} e_x \\ e_y \\ e_s \end{bmatrix} \quad (4.18)$$

Where $[S]_{x,y}^k$ $[\sigma]_{x,y}^k$ are the strains produced by the existing stresses in the lamina. The following relation given in equation 4.19 can obtain the stresses in any layer in a laminate with respect to global co-ordinate axis.

$$\begin{bmatrix} \sigma_x \\ \sigma_y \\ \tau_s \end{bmatrix} = \begin{bmatrix} Q_{xx} & Q_{xy} & Q_{xs} \\ Q_{yx} & Q_{yy} & Q_{ys} \\ Q_{sx} & Q_{sy} & Q_{ss} \end{bmatrix} \begin{bmatrix} \varepsilon_x - e_x \\ \varepsilon_y - e_y \\ \gamma_s - e_s \end{bmatrix} \quad (4.19)$$

4.6.1 Radiator Problem Definition

The radiator panel, apart from structural requirements, is also required to dissipate 100 watts/m^2 to space from the electronics box during flight. The setup for the radiator panel is shown in Figure 4.8, where the coolant passes through the electronics box takes the heat from it and transfers it to the core at the midplane. Therefore the performance of the radiator is tested by placing the heat load at the mid-plane of the core and allowed to conduct and radiate on one side of the panel, while the other side is not exposed. The corresponding model is presented in the Figure 4.9.

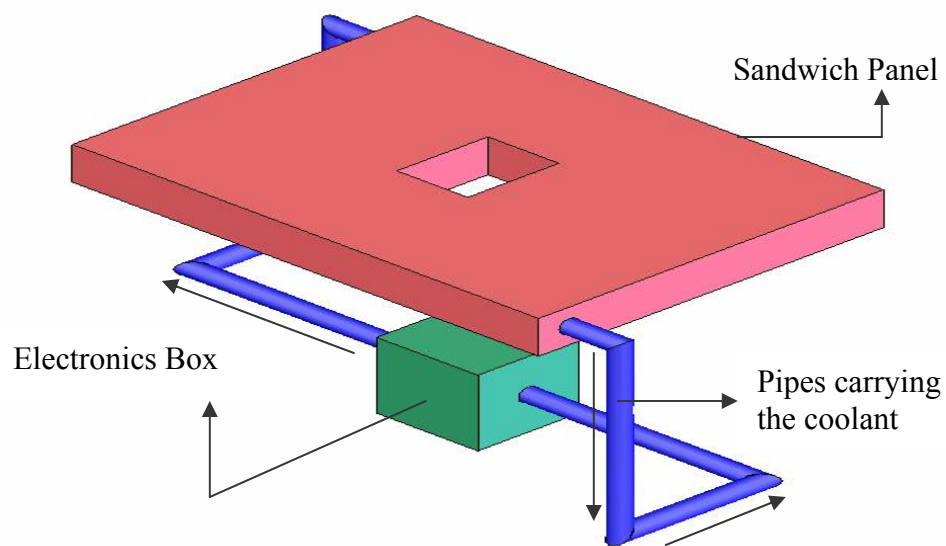


Figure 4.8. Schematic representation of the heat removal system from the electronics box.

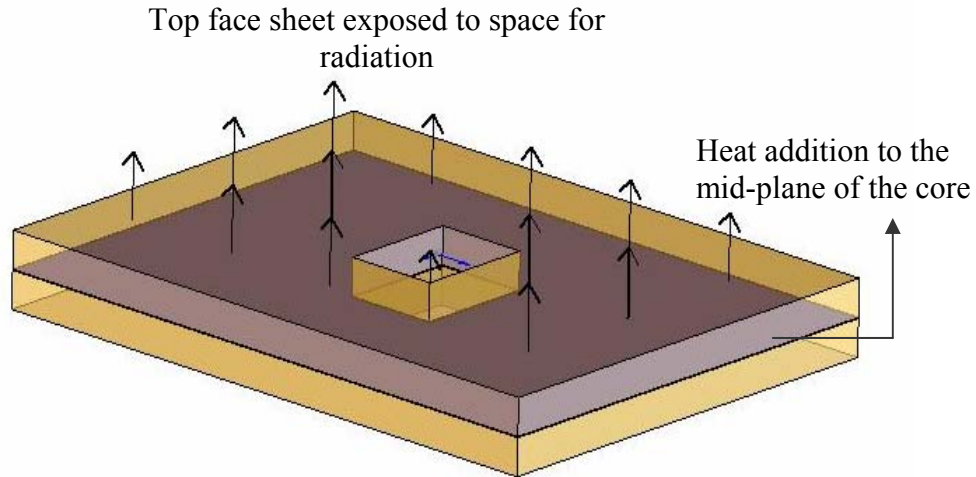


Figure 4.9. Schematic representation of heat loads modeled in MSC Nastran.

The ambient temperature of the space is assumed to be 250° Kelvin if the radiator panel is at International Space Station or 4° Kelvin, if it is radiating to deep space [27]. But in this case it is assumed to be 250° Kelvin. The emissivity and absorptivity of the surface exposed to radiation is assumed to be 0.8. The radiator panel consists of sandwich composite with two carbon epoxy face sheets on either side of the core. The choice of the core is made by extensive heat transfer analysis both steady state and transient. The core that satisfies the thermal requirements with better performance is determined. The lay-up that satisfied the structural requirements in section 5.1 is considered for thermal analysis to verify that it is able to satisfy the thermal requirements of the radiator panel. As the face sheet thicknesses are very small, it is assumed that the face sheets will not conduct heat significantly. Therefore much of the design and analysis is dependent on the material and the thickness of the core.

4.6.2 Core Materials and Support Conditions

Poco Graphite Inc. offers two thermal management materials Poco foam and Poco foam HTC. Both are cellular graphite foams that have very high thermal conductivity in the out of plane direction. Poco foam HTC has higher strength and thermal conductivity than the Poco foam. However, its higher density increases the weight of the system and might incidentally reduce the performance of the system. Aluminum Honeycomb is also a potential choice for the core of the radiators. It is very lightweight and has high stiffness characteristics. The thermal conductivity of aluminum honeycomb is lesser than its parental aluminum due to the hexagonal arrangement of cells. The sandwich panel is supported on all sides. The boundary conditions for the thermal problem will be similar to the vibration. All the nodal degrees of freedom on the thickness of the panel are fixed.

4.6.3 Thermal Modeling using MSC Nastran

MSC Nastran is the widely used code for structural analysis of components. This program also has a thermal analysis part, which is based on the “Finite Element method” (FE). The primary function of the radiator panel is to dissipate the 100 W/m^2 of heat flux from the electronics box to space. The heat flux load is defined at the mid-plane of the core and it is allowed to conduct through the sandwich and radiate to the surrounding space through one side of the composite panel. Since the other side of the composite panel is not exposed, it is not able to radiate. The choices that are available in MSC Nastran to define the heat flux load on the panel are; specifying it as nodal load or specifying it as element load. Heat flux and heat generation can be defined on both nodes and elements. The units for the nodal heat generation and heat flux are both expressed in terms of power units instead of the more traditional units used by the element heat generation and heat flux. The difference is due to the fact that nodes have neither a volume nor an area whereas the element has. As shown in the figure 4.12, the heat generation and heat flux loads can vary with time.

4.6.3.1 Thermal Units

The nodal and elemental loads have the following units for temperature, heat generation and heat flux in MSC Nastran. This is shown in Figure 4.10.

Nodal Loads		Elemental Loads	
Temperature	°C, °K, °F, °R	Temperature	°C, °K, °F, °R
Heat Generation	W, Btu/sec	Heat Generation	W/m ³ , Btu/sec-in ³
Heat Flux	W, Btu/sec	Heat Flux	W/m ² , Btu/sec-in ²

Figure 4.10. MSC Nastran units for heat loads. [21]

For the problem at hand, the heat flux loads are specified as nodal loads at the mid plane of the core by selecting all the nodes at that plane. The number of nodes at the mid-plane of the core is 3686. As the panel is modeled in inches, the heat flux loads assume the form BTU/sec. The total heat flux of 100 W/m² after conversion becomes 2.657E-5 BTU/sec on a single node. The units of temperature in this problem are in Rankin. This is because the unit of Stefan Boltzmann constant is expressed either in W/m²/K⁴ or BTU/h-ft²-R⁴. This load form with the nodal load is shown in Figure 4.11.

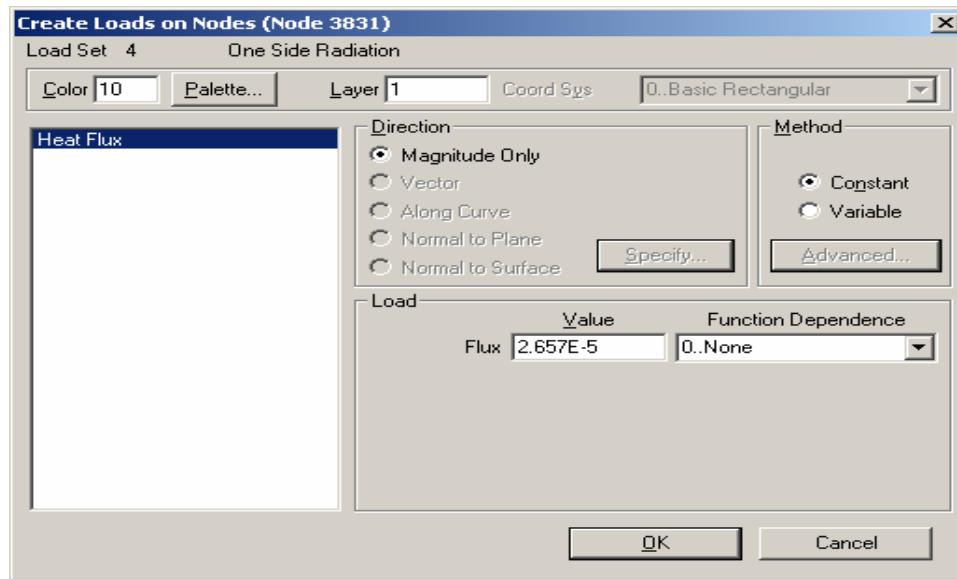


Figure 4.11. Nodal heat load form in MSC Nastran.

4.6.3.2 Radiation to Space

This problem involves radiation only on one side of the composite panel. The radiation to space is considered to be a boundary condition that involves radiant exchange between a panel and a blackbody space. The parameters that are required for the radiation to space are as follows

- The absorptivity and emmissivity of the radiating surface,
- Ambient temperature of space and
- Radiation view factor between surface and space, which is generally equal to one.

The absorptivity and emmissivity can be both temperature dependent and the ambient temperature can also vary with time. In this analysis, the absorptivity and emmissivity is assumed to be 0.8 and ambient temperature of the space is assumed to be 250⁰K. The relationship that involves radiation is defined to be

$$q = \sigma * viewfactor * (\varepsilon * T_s^4 - A * T_{amb}^4) \quad (4.20)$$

q = net heat energy involved in W/m^2

ε = Emmisivity of the radiating surface

A = Absorptivity of the radiating surface

T_s = Temperature of the element at the radiating surface.

T_{amb} = Temperature of the ambient space and

σ = Stefan Boltzmann constant which has the value $5.668E-8 W/m^2/K^4$ or $0.1714E-8 BTU/h-ft^2-R^4$. The constant is calculated to be $3.31E-15 BTU/sec-in^2-R^4$ and is used in the analysis.

The equation is inherently non-linear due to the presence of the fourth power in the radiation term. MSC Nastran applies Newton-Raphson iteration scheme for the solution of these non-linear equations.

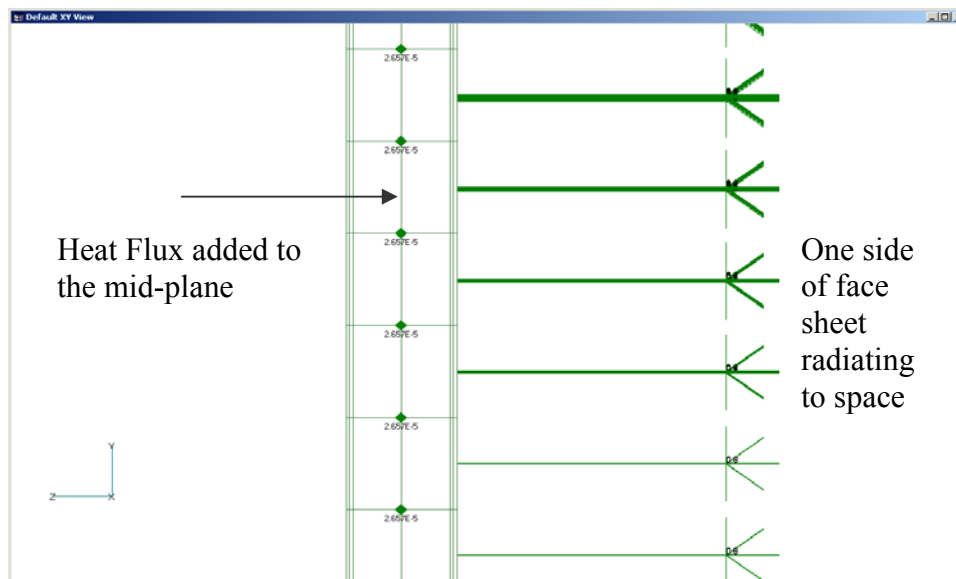


Figure 4.12. Sandwich panel with heat flux and radiation. (MSC Nastran)

The side view of the radiator panel in Figure 4.12 identifies the nodal heat loads at the mid plane of the core as dots with the values next to it. The radiation is only on one side of the panel shown with arrow marks. A steady state heat transfer analysis is performed in Nastran with this model. Since it is steady state analysis, temperature does not depend on time where in transient heat transfer analysis, heat input is given as function of time. This is discussed at the later part of this chapter.

4.6.4 One Dimensional Steady State Heat Transfer

Temperature distribution in the sandwich panel

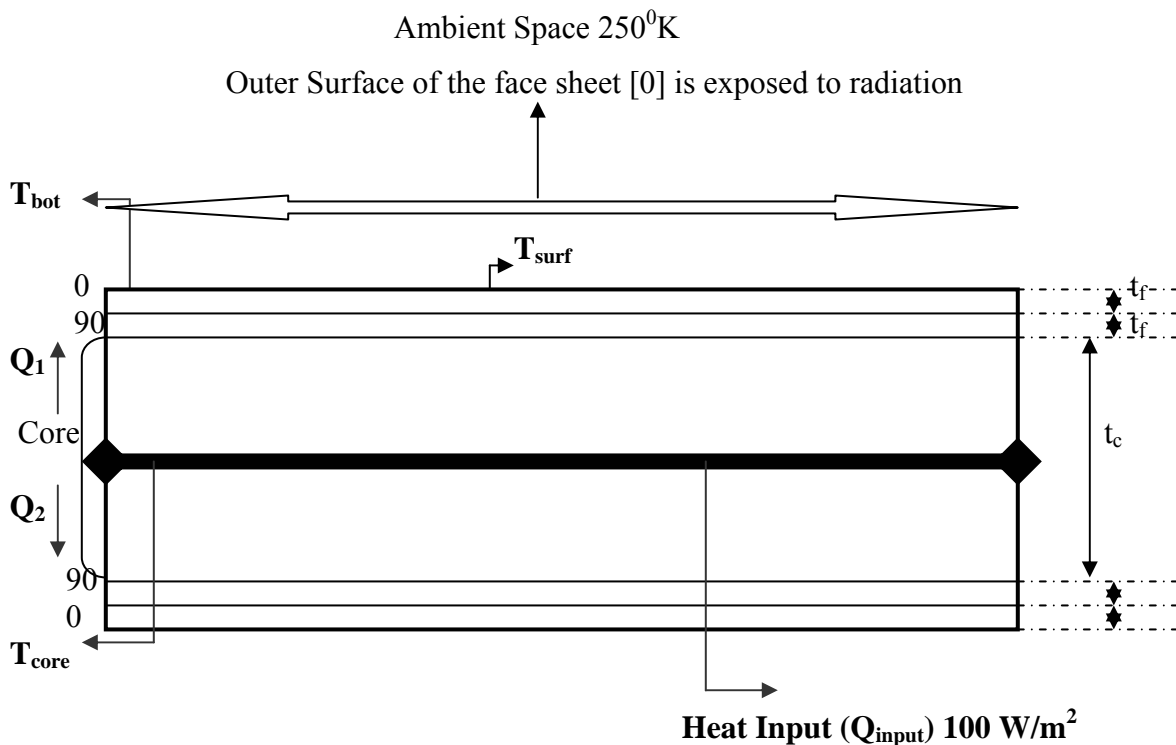


Figure 4.13. One-dimensional analytical model for temperature field.

To begin with, assume the sandwich panel has heat load input in the middle and both the sides are exposed to radiation. The schematic of one-dimensional thermal model is shown in the Figure 4.13.

$$Q_{\text{input}} = Q_1 + Q_2. \quad (4.21)$$

Since $Q_{\text{input}} = 100 \text{ W/m}^2$. Due to symmetry, $Q_1=Q_2=50 \text{ W/m}^2$. As the cross sectional area of the radiator panel is approximately 1 m^2 , the heat input (Q_{input}) is 100 W.

$$Q_1 = Q_{\text{conduction}} + Q_{\text{radiation}} \quad (4.22)$$

$$Q_1 = (T_{\text{core}} - T_{\text{surf}}) / ((t_c / (2 * K_{\text{core}})) + (t_f / K_{\text{fs}})) + \epsilon * A * \sigma * (T_{\text{surf}}^4 - T_{\text{ambient}}^4) \quad (4.23)$$

Where σ = Stefan Boltzmann Constant

A = Area of the panel

ϵ = Emmisivity of the surface (assumed to be 0.8)

There are two unknowns in this equation T_{core} and T_{surf} .

For steady state heat transfer $Q_{\text{conduction}} = Q_{\text{radiation}}$

So considering the radiation part alone,

$$Q_{\text{radiation}} = \epsilon * A * \sigma * (T_{\text{surf}}^4 - T_{\text{ambient}}^4) \quad (4.24)$$

Here $Q_{\text{radiation}} = 50 \text{ Watts}$

The panel is 46X34 inches and it has a cut out of 7X9 inches.

$$\text{Area} = ((46 * 34 - 7 * 9) * 0.0254^2) = 0.96839 \text{ m}^2.$$

Stefan Boltzmann constant (σ) = $5.67 \text{e-}8 \text{ Watts/m}^2 \cdot \text{k}^4$

$$T_{\text{surf}} = [(Q_{\text{radiation}} / (\epsilon * A * \sigma)) + (T_{\text{ambient}})^4]^{1/4} \quad (4.25)$$

$$T_{\text{surf}} = [50 / (0.8 * 0.96839 * 5.67 \text{e-}8) + 250^4]^{1/4} \quad (4.26)$$

$$T_{\text{surf}} = \mathbf{266.50^\circ\text{K}} \quad (4.27)$$

Conduction in the face sheets (Through the thickness)

$Q_{\text{conduction}} = 50\text{Watts}$. The thermal conductivity utilized for this calculation is that of the matrix because the through the thickness direction is dominated by matrix.

$$Q_{\text{conduction}} = K_{\text{matrix}} * A (T_{\text{bot}} - T_{\text{surf}}) / t_f \quad (4.28)$$

$$50 = 0.4135 * 0.96839 (T_{\text{bot}} - 266.50) / (0.2 * 0.0254) \quad (4.29)$$

$$T_{\text{bot}} = 183.68 + 0.63425 = 267.13^\circ\text{K} \quad (4.30)$$

Conduction in the core (Through the thickness)

$$Q_{\text{conduction}} = 50\text{Watts}$$

$$Q_{\text{conduction}} = K_{\text{core}} * A (T_{\text{core}} - T_{\text{bot}}) / t_c \quad (4.31)$$

$$50 = 135 * 0.96839 (T_{\text{core}} - 267.13) / (0.3 * 0.0254) \quad (4.32)$$

$$T_{\text{core}} = 267.13 + 0.0025 = 267.13^\circ\text{K} \quad (4.33)$$

The above calculation is based on the assumption that the panel is radiating on both the sides of the composite panel. Therefore preliminary calculations can be made for the panel with one side radiation. This calculation yields a reasonable good estimate of the temperature at the surface that is radiating.

If only one side of the panel is radiating, then a reasonable approximation for a steady state heat transfer analysis would be to radiate the 100 watts of heat to the space instead of 50 watts. This calculation is shown below. Considering again the radiation part alone,

$$Q_{\text{radiation}} = \epsilon * A * \sigma * (T_{\text{surf}}^4 - T_{\text{ambient}}^4) \quad (4.34)$$

So here $Q_{\text{radiation}} = 100$ Watts

$$T_{\text{surf}} = [(Q_{\text{radiation}} / (\epsilon * A * \sigma)) + (T_{\text{ambient}})^4]^{1/4} \quad (4.35)$$

$$T_{\text{surf}} = [100 / (0.8 * 0.96839 * 5.67E-8) + 250^4]^{1/4} \quad (4.36)$$

$$T_{\text{surf}} = \mathbf{280.41^\circ K} \quad (4.37)$$

The surface temperature calculated with above assumptions has good agreement with the surface temperature from Nastran after the steady state heat transfer analysis. The one dimensional steady state heat transfer calculation not only provides the temperature distribution in the panel but also proves the fact that through the thickness variation is very much dependent on the thermal conductivity of the material. The above calculation provides us an interesting fact that there is no difference in temperature between the T_{bot} and T_{core} . T_{bot} is the surface temperature at the core and T_{core} is the mid-plane temperature of the core.

4.6.5 Thermal Stresses [6]

An estimate of thermal stresses is made by approximating the sandwich panel to be a beam. For a beam that is made of single ply isotropic material or a unidirectional composite material, the equation 4.38 gives the total stress that includes both mechanical and thermal loads.

$$\sigma_x = \frac{1}{A}(P + P^T) + \frac{Z}{I}(M + M^T) - E\alpha\Delta T \quad (4.38)$$

Where

P = Mechanical Load and

M = External Moment applied.

P^T = Thermal load.

M^T = moments induced due to thermal loads.

Z = Section Modulus

I = Moment of Inertia.

Now consider the sandwich panel rigidly fixed on all the sides, i.e. the panel cannot expand on heating. Since the displacement is zero, the strain is also zero.

$$\varepsilon_x = \frac{du_0}{dx} = 0 \quad (4.39)$$

The governing differential equation

$$P + P^T = EA \frac{du_0}{dx} \text{ yields} \quad (4.40)$$

$$P = -P^T \quad (4.41)$$

Assuming there is no beam bending $M_b = 0$ and because of uniform heating $M^T = 0$, the stress equation 4.38 becomes

$$\sigma_x = -E\alpha\Delta T \quad (4.42)$$

In general, the thermal analysis of any structure is very involved due to the complications in calculating the thermal strains, the non-homogeneous boundary conditions and anisotropic material behavior of the structure. Therefore the generalization that there will be no thermal stresses if the structure is free to expand and if the structure is held rigidly, thermal stress from equation 4.42 can always be made. Considering the Poisson ratio effects, the worst case stress is $\sigma_x = -E\alpha\Delta T / (1 - \nu^2)$. As a preliminary design and to find out if thermal stresses affect the stability of the structure, this calculation for the largest value of E and highest value of ΔT will provide

the maximum value of thermal stress that the structure can withstand. The reference temperature is assumed to be 294⁰K. The temperature difference (ΔT) is obtained from steady state temperature discussed in section 4.6.4. The unit of temperature in equation 4.44 is rankine.

Case 1: When both the face sheets are exposed to radiation

Thermal Stress (σ) in the core is given by the equation 4.44.

$$\begin{aligned}
 (\sigma)_{\text{Core max}} &= - ((E_{\text{Core}}) * (\alpha)_{\text{Core}} * (\Delta T)_{\text{max}} / (1 - \nu^2)) & (4.43) \\
 &= - (5801.6 * 1.11\text{e-}06 * (480.8 - 529.2) / (1 - 0.4^2)) \\
 &= \mathbf{0.37 \text{ Psi}}
 \end{aligned}$$

Case 2: When one of the face sheets is exposed to radiation

Thermal Stresses (σ) in the core is given by the following formula

$$\begin{aligned}
 (\sigma)_{\text{Core max}} &= - ((E_{\text{Core}}) * (\alpha)_{\text{Core}} * (\Delta T)_{\text{max}} / (1 - \nu^2)) \\
 &= - (5801.6 * 1.11\text{e-}06 * (504.7 - 529.2) / (1 - 0.4^2)) \\
 &= \mathbf{0.19 \text{ Psi}}
 \end{aligned}$$

To evaluate the thermal stresses in the face sheets, the panel is analyzed in a commercial code Laminator, a product based on Classical laminate plate theory. The results of the code Laminator and their stress comparisons with Nastran are discussed in the final chapter Numerical Results and Discussion

4.6.6 Transient Heat Transfer Problem

In the steady state heat transfer analysis, there was no time dependency factor involved in solving the equations. The most general form of steady state heat balance is given by equation 4.44.

$$[K]\{u\} + [R]\{u + T_{abs}\}^4 = \{P\} + \{N\} \quad (4.44)$$

This equation is inherently non-linear due to the presence of the radiation term or temperature dependent properties and boundary conditions. MSC Nastran for Windows performs simulation of linear, non-linear, steady state and transient thermal systems with relative ease due to its adaptive solution strategy. This equation pertains to non-linear steady state heat balance equation, as it does not involve time factor. In order to predict the time effect on the performance of the radiator panel, transient heat transfer analysis is performed on this problem. This analysis will provide us an estimate for the time taken for the radiator panel to attain steady state, that is, after which whatever heat is supplied in is dissipated to the surrounding space. This necessitates knowing the general form of non-linear transient heat balance given by the equation 4.45

$$[B]\{\dot{u}\} + [K]\{u\} + [R]\{u + T_{abs}\}^4 = \{P\} + \{N\} \quad (4.45)$$

Where,

[K]- Heat Conduction Matrix

[R]- Radiation Exchange Matrix

\{u\}- Vector of unknown temperatures

T_{abs}- Temperature offset from absolute, used in radiation

\{P\} – Vector of constant applied heat flows

\{N\} – Vector of temperature dependent heat flows

[B] – Heat capacity matrix

$$\{\dot{u}\} - du/dt$$

This equation, due to its transient behavior, must be integrated with time. The time integration is performed using the Newmark's numerical method. Non-linear iterations are also required for the solution of this equation.

Analysis condition in Nastran

Transient analysis requires certain conditions to be input before the run time. The total solution time needs to be specified by the user. The user provides the initial time step and the total number of time steps and Nastran calculates the total solution time. The actual time step used by Nastran may be different than that of the user as it employs adaptive solution strategy. To avoid errors in convergence or inaccurate results, correct estimate of the time step is required.

The Nastran form with the analysis conditions pertaining to transient analysis of radiator panel is shown in Figure 4.14.

Figure 4.14. Transient analysis form in MSC Nastran.

To verify the results of transient analysis from Nastran, an analytical model is built in Maple 8.0 [28]. To simplify the calculation, only core is considered for the transient analysis. The core materials are Poco foam and aluminum honeycomb. A plot has been generated between surface temperature and time. As this involves the assumption of using core alone, the surface temperature from the analytical model can be compared with the results from Nastran.

4.6.7 Orbit Analysis of Radiator Panel in Space

Orbits:

Low Earth Orbit (LEO)

This orbit has maximum altitude <1852 Km

Geosynchronous orbit (GEO)

This orbit has very low inclination and altitude of 36000 km. The period matches the rotation of the earth and therefore the space object appears to be at the same spot from the earth.

Middle Earth Orbit (MEO)

It has an altitude less than GEO and greater than that of the LEO.

Molniya

This orbit is highly inclined and elliptical.

Out of the above-mentioned four orbits, LEO and GEO are considered to be important. The radiator panel apart from dissipating the heat from the electronics receives various heat loads from the environment. They are categorized as following.

a) **Solar**: This refers to heat flux received from the sun. This is given by

$$A \cdot \alpha \cdot (\text{Solar constant})$$

b) **Albedo**: It is the percentage of heat flux that is reflected back to space from the earth and it is dependent on the altitude. It is given by

$$A \cdot \alpha \cdot (\text{Albedo})$$

c) **Earth's IR**: This heat load is emitted by the earth with much higher wavelength and cannot be avoided by thermal coatings since the same coating would prevent the radiation of heat loads from the electronics. Therefore this heat load can create a heavy back load on radiators. This is given by

$$A \cdot \epsilon \cdot (\text{IR})$$

$$\text{Total heat load in LEO} = A \cdot \alpha \cdot (\text{Solar constant}) + A \cdot \alpha \cdot (\text{Albedo}) + A \cdot \epsilon \cdot (\text{IR}) \quad (4.46)$$

$$\text{Total heat load in GEO} = A \cdot \alpha \cdot (\text{Solar constant}) \quad (4.47)$$

The equations 4.46 and 4.47 give an idea on the parameters to be taken care in choosing the orbit. It is of interest to investigate the behavior of the core material to the incident of heat loads from the sun. A simple flat plate representing the radiator panel is built in Thermal desktop version 4.5 [31]. The panel follows the **LEO**. The analysis in general compares the performance of Poco foam and Aluminum honeycomb material, as they are considered to be potential choices of the core material. It is to be noted that aluminum honeycomb material has the same specific heat capacity as that of aluminum. The following assumptions are made to carry out the analysis.

- The radiator panel mass is assumed to be 25 Kg.
- Specific heat capacity C_p of Aluminum = 900 J/kg-K
- Specific heat capacity C_p of Poco foam = 700 J/kg-K
- Density of Aluminum = 2770 Kg/m³
- Density of Poco foam = 550 Kg/m³

From the analysis the maximum temperature experienced by the two materials due to the environment loads are predicted. This prediction is a good measure of the efficiency of the core material to draw the heat from the electronics box assembly.

CHAPTER V

NUMERICAL RESULTS AND CONCLUSIONS

5.1 Finite Element Modal Results of Plates and Sandwich Composites

In the previous chapters, a baseline radiator panel design, where finite element models were setup through material, element selection and application of boundary conditions to parametrically study the free vibration and thermal response of the sandwich panel, is proposed and discussed. Therefore it is indeed important to discuss and interpret the finite element analysis results of the radiator panel that is implemented in critical areas of spacecraft. It is also essential to evaluate the heat transfer capabilities of the core of the radiator panel. The selection of the core material, as discussed, is an important factor in the thermal aspect of the radiator. This is well established in the finite element analysis results of the sandwich radiator panel with different types of core. Apart from the existing setup for thermal model, a distinct approach is proposed to clearly identify the efficiency of the radiator and to select the material of the core. As the design and optimization of the sandwich panel proceed sequentially, at first the free vibration results of the panel are presented. Then based on the fundamental frequency results, optimization of the parameters such as thickness, lay-up and orientation is performed and then with the optimized model the static, dynamic and thermal analysis results of the radiator panel are presented. In section 4.3, a parametric study on the free vibrations of isotropic, orthotropic plates and sandwich configurations is discussed. In that section it is assumed to have pinned edges for the sandwich panel. This assumption is only for validation purposes and does not represent the true conditions of the radiator panel. The closed form solution is presented in section 4.3 using Maple version 8.0 [28] along with graphical representation of the variation of the fundamental frequency with parameters of sandwiches. It is necessary to compare the numerical values from closed form solution with MSC Nastran results. In the Figures 5.1-5.3, the mode shapes of the plates

and sandwiches that are considered for parametric study are presented here. A comparison of two solution forms is also presented in Table 5.1.

Mode shapes of plates and sandwiches

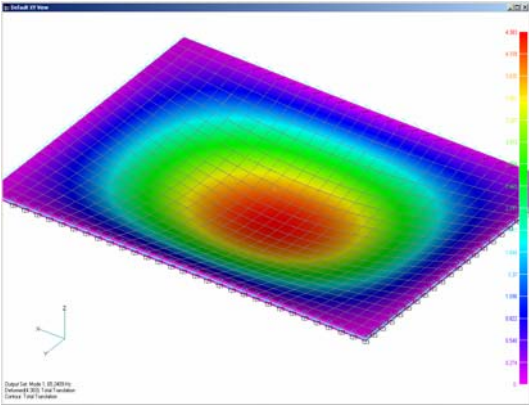


Figure 5.1. Isotropic plate.

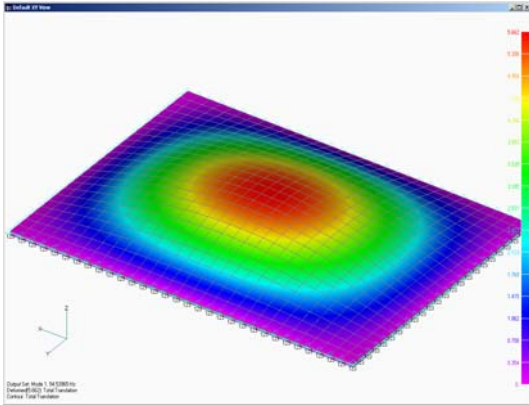


Figure 5.2. Specially orthotropic laminate [0/90/90/0].

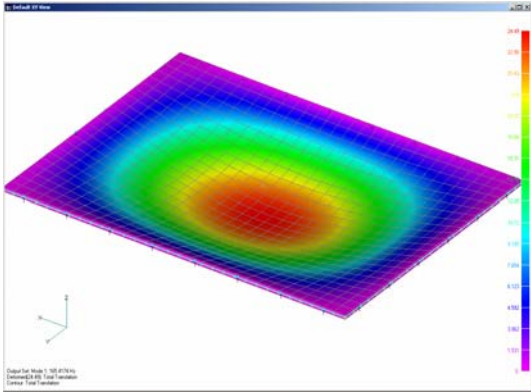


Figure 5.3. Sandwich plate [0/90/core/90/0].

Table 5.1

Modal comparison between MSC Nastran and analytical solution.

Plate Configuration	Material	Boundary condition	Thickness of the plate (Inches)	CLPT Equation	MSC Nastran	% Error	
Isotropic Plate	Aluminum 2024 – T3	All edges pinned	0.51	65.655	65.241	<1	
Specially Orthotropic Plate [0/90/90/0]	T300/5208 carbon epoxy	All edges pinned	0.51	54.645	54.539	<1	
Sandwich Plate [0/90/core/90/0]	Face sheet T300/520 8 carbon epoxy	Core Foam core	Face sheet 0.005	Core 0.5	161.379	163.064	<2

5.2 Free Vibration Results of Sandwich Radiator Panel

It is clear from the Table 5.1 that MSC Nastran predictions are in good agreement with the closed form solution for the given material properties, boundary conditions and all the parameters such as thickness of the face sheets and core considered. The table also suggests that [0/90/core/90/0] lay-up is considered to provide sufficient stiffness to the panel. Even though the face sheets are of carbon/epoxy and core is of foam type, the elastic and thermal properties need to be updated for the three dimensional analysis. Unlike the parametric study, the three dimensional model has a cut out in the middle and has an antenna mass in it. This demands an increase in the thickness of the face sheets and therefore with the updated properties of T300/5208 carbon epoxy face sheets and core materials of Poco foam and aluminum honeycomb, the following lay-up and thicknesses are considered for further analysis.

Lay-up considered – [0/90/core/90/0]

Thickness of each face sheet – 0.1 inch

Thickness of the core – 0.6 inch

Material of the face sheet – T300/5208 carbon epoxy

Material of the core – Poco foam, Poco foam HTC and Aluminum honeycomb

Table 5.2

Modal results of sandwich panel with different types of core.

			Units	Aluminum Honeycomb	POCO Foam	POCO Foam HTC
Properties	Young's Modulus (E)	E₁₁	PSI	3.77E+04	5.80E+04	5.80E+04
		E₂₂		4.52E+04	5.80E+04	5.80E+04
		E₃₃		2.01E+05	5.80E+04	5.80E+04
	Shear Modulus (G)	G₁₂	PSI	15000	20720	20720
		G₂₃		58000	20720	20720
		G₁₃		15000	20720	20720
	Poisson's Ratio (ν)	ν₁₂		0.33	0.4	0.4
	Expansion Coefficient (α)	a₁₁, a₂₂	in/in-R	1.32E-05	3.40E-07	5.70E-07
		a₃₃		1.32E-05	-3.90E-07	-5.90E-07
	Thermal Conductivity (K)	K₁₁	Btu/in-sec-R	2.47E-05	0.0006	0.00094
		K₂₂		1.65E-05	0.0006	0.00094
		K₃₃		4.39E-05	0.0018	0.0033
	Specific Heat Capacity (C_p)	(C_p)	Btu/lb-R	0.2151	0.17	0.17
			J/g-K	0.9	0.7	0.7

Table 5.2 Continued

	Density (p)	ρ	lb-sec²/inch⁴	3.45E-06	5.10E-05	8.42E-05
MODAL ANALYSIS	Mode 1		Hz	220	173.96	164.17
	Mode 2		Hz	414	341.83	310.11
	Mode 3		Hz	532	400.78	363.61
	Weight of radiator panel		Kg	16.881	24.37	29.62

It is evident from Table 5.2 that aluminum honeycomb due to its high stiffness, has the highest fundamental frequency compared to Poco foam cores. Also the weight of the panel suggests that aluminum core sandwich panel weighs much less than Poco foam core panel. At this stage, it is difficult to suggest the material of the core since the radiator panel needs to be analyzed for its thermal loads. But the above results show the need for optimization of the parameters of the sandwich, as excess stiffness is associated with it.

5.2.1 Structural Optimization and Vibration Results of Radiator Panel

As found in the Table 5.2, the panel with the above mentioned lay-up and thickness has excess rigidity associated with it meaning higher fundamental frequency. Since the requirement suggests that fundamental frequency of the radiator panel be above 100 Hz, it is necessary to select the proper orientation and thickness of the components of the sandwich to be just able to meet the fundamental frequency requirement. But the lay-ups mentioned in the previous section provide fundamental frequency that is much greater than 100 Hz and therefore the need for optimization. In this section, the structural optimization is discussed and the optimized panel meeting the structural requirements is presented. The radiator panel with different combination of lay-up and orientation is analyzed in MSC Nastran and the modal results are presented as follows. This is shown in Table 5.3.

Table 5.3

Fundamental frequencies of cross-ply lay-ups for radiator panel.

Lay-up	Classification	Fundamental mode (MSC Nastran)
0/0/core/0/0	Symmetric laminate	147.47 Hz
0/90/core/90/0	Symmetric Cross ply laminate	173.96 Hz
90/0/core/0/90	Symmetric Cross ply laminate	188.07 Hz
90/90/core/90/90	Symmetric Laminate	180.05 Hz
0/90/core/0/90	Anti symmetric cross ply laminate	180.37 Hz
90/0/core/90/0	Anti symmetric cross ply laminate	180.38 Hz

This panel in Table 5.3 utilizes Poco foam properties for the core of the radiator panel. Even though [90/0/core/0/90] provides higher stiffness, it is not phenomenal. Further the optimization is pursued by changing the stacking sequence of the face sheets.

Thickness of the face sheet - 0.01 inch (reduced by order of 10)

Thickness of the core – 0.6 inch

Material of core – Poco foam

Material of face sheet – T300/5208 carbon epoxy

The following lay-ups are shown in Table 5.4.

Table 5.4

Fundamental frequencies of angle ply lay-ups for radiator panel.

Lay-up	Fundamental frequency
0/90/core/90/0	111 Hz
15/-15/core/-15/15	109 Hz
45/-45/core/-45/45	104 Hz
60/-60/core/-60/60	108 Hz
75/-75/core/-75/75	112 Hz
90/90/core/90/90	117 Hz
90/0/core/0/90	114 Hz

Thus the optimum stacking sequence from the Table 5.4 is cross-ply with the same number of 0° and 90° plies. Incidentally it is also proven that an angle ply laminate is never better than a cross-ply or unidirectional laminate in the aspect of increasing the stiffness [31]. Based on the results, it can be stated that changing the orientation does not give a good chance or reducing the weight of the panel. The increase in the fundamental frequency due to the change in orientation of the fibers is not substantial. (< 10 Hz). Therefore the optimized lay-up for the composite face sheets is remained as 0/90/core/90/0. This configuration provides fundamental frequency greater than 100 Hz.

After determining the optimized stacking sequence for the face sheets of the radiator panel, it is necessary to find out the optimized thickness. The following lay-up with Poco foam is considered for the analysis. The lay-up represents the thickness of 0/90/core/90/0. All units are in inches.

- 0.01/0.01/1.0/0.01/0.01

The fundamental frequency is found to be 116 Hz. The weight of the panel is 15 Kg. This lay-up is assumed to be the optimized for Poco foam core until further analysis. Knowing the fact that the density of the aluminum honeycomb is much less compared to Poco foam, the weight of the optimized panel with aluminum honeycomb core is expected to be very low. Now with aluminum honeycomb core, the following configuration is considered for the analysis.

- .01 / 0.01 / 1.0 / 0.01 / 0.01

The fundamental frequency is found to be 148 Hz. This shows that there is much scope for optimization to provide the best lay-up. Now the following lay-up is considered.

- 0.01 / 0.01 / 0.6 / 0.01 / 0.01

The fundamental frequency for this lay-up is very close to 100 Hz. Therefore proceeding with a higher thickness, consider

- **0.01 / 0.01 / 0.7 / 0.01 / 0.01**

The fundamental frequency is found to be 116 Hz. It is very close to the optimized panel with aluminum honeycomb as core of the sandwich. The weight of the panel is found to be **2.27** Kilograms. Now the optimized panels for Poco foam and aluminum honeycomb are compared. It is clear that the thickness of the core with Poco foam should be less than the thickness of the core with aluminum honeycomb to have an optimized model. Hence

- 0.02 / 0.02 / 0.5 / 0.02 / 0.02

lay-up is considered. The fundamental frequency is 91 Hz. To make it above 100 Hz,

- **0.02 / 0.02 / 0.6 / 0.02 / 0.02**

lay-up is considered. The fundamental frequency is **111 Hz** and the weight of the panel is **11.30 Kilograms**. As Poco foam HTC is denser than Poco foam, the fundamental frequency of the same panel with foam HTC will be lesser than the one with Poco foam but still meeting the requirement of 100 Hz.

Table 5.5

Fundamental frequencies of the optimized radiator sandwich panel.

Lay-up	Thickness of the face sheets and core	Core Material	Boundary Conditions	Fundamental frequency (Hz)	Weight of the sandwich panel (Kg)
[0/90/core/90/0]	[0.01 / 0.01 / 0.7 / 0.01 / 0.01]	Aluminum Honeycomb	All sides fixed	116	2.27
[0/90/core/90/0]	[0.02 / 0.02 / 0.6 / 0.02 / 0.02]	Poco foam	All sides fixed	111	11.30
[0/90/core/90/0]	[0.02 / 0.02 / 0.6 / 0.02 / 0.02]	Poco foam HTC	All sides fixed	104	16.55

The modal results for optimized panels with different cores are presented in Table 5.5. The mode shapes of the above-determined optimized panels are presented in the following section.

5.2.2 Free Vibration Mode Shapes

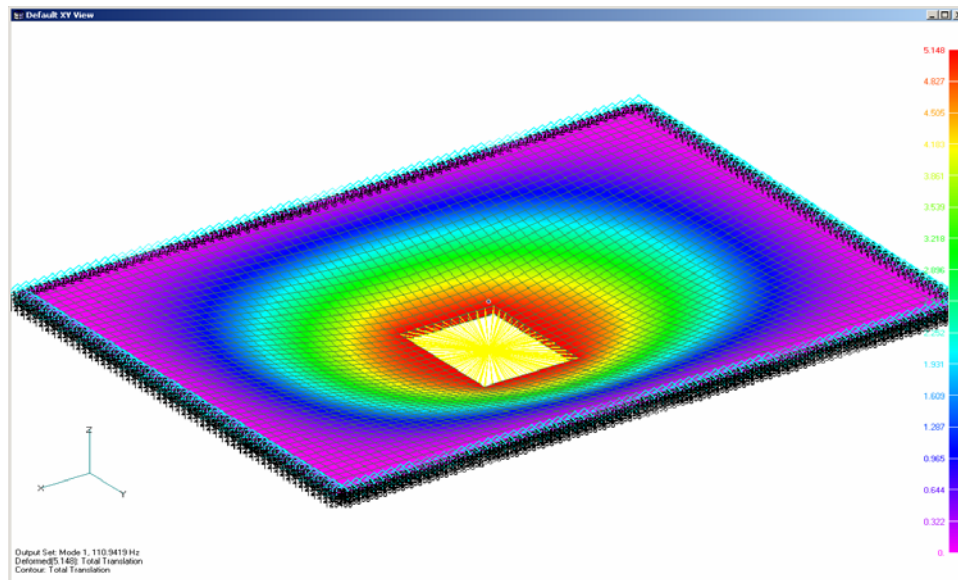


Figure 5.4. Fundamental mode shape of the Poco foam sandwich radiator panel.

As the mode shapes of the radiator panel with cores of Poco HTC and aluminum honeycomb take the same profile as of Figure 5.4, it is not presented here. It should be noted that the fundamental frequency for the panel varies with the stiffnesses of the core. Aluminum honeycomb has higher elastic properties compared to Poco foam and Poco foam HTC and therefore it is reflected in a high fundamental frequency of the panel. As the density of the aluminum honeycomb is lesser than Poco foam, the panel is expected to have very low weight among the three cores. The Table 5.5 suggests that aluminum honeycomb core panel provides the best configuration with least weight among the cores. But it is of interest to know that if the panel with aluminum honeycomb core will be able meet the thermal requirements since Poco products possess high thermal

conductivity. This summarizes the vibration results of the panel with different types of cores. With the results, it is understood that Poco products do not perform better than aluminum honeycomb.

5.3 Static and Dynamic Analysis of Sandwich Radiator Panel

The selected radiator panels have satisfied the requirements for fundamental frequency and therefore it is now necessary for the panel to withstand the stresses due to static and dynamic gravitational loads experienced during launch and descent of the spacecraft. The source and the calculation of dynamic loads are discussed in detail in the section 4.5.3. As the dynamic loads exceed the static load of 10G, it is more reasonable to predict the stress and deformation characteristics of the radiator panel for dynamic loads. The dynamic loads are calculated based on the fundamental frequency of the panel. The random vibration loads for the sandwich panel with three types of cores on all the coordinate directions can be found in Tables 5.6, 5.7 and 5.8.

5.3.1 Dynamic Load Sets

These dynamic loads are different for each panel as they depend on the fundamental frequency and they are higher for stiffer panel. These are provided as static body loads to the panel in inch/sec^2 in accordance with the units in MSC Nastran.

Table 5.6

Dynamic loads for sandwich panel with Poco foam as core.

Load Sets (g's)	X Axis	Y Axis	Z Axis
Set 1	32.95	5.90	6.30
Set 2	7.90	30.95	6.30
Set 3	7.90	5.90	31.35

Table 5.6 Continued

Load Sets (in/sec²)	X Axis	Y Axis	Z Axis
Set 1	12733.33	2279.76	2434.32
Set 2	3052.56	11960.53	2434.32
Set 3	3052.56	2279.76	12115.09

Table 5.7

Dynamic loads for sandwich panel with Poco foam HTC as core.

Load Sets (g's)	X Axis	Y Axis	Z Axis
Set 1	32.15	5.90	6.30
Set 2	7.90	30.15	6.30
Set 3	7.90	5.90	30.55
Load Sets (in/sec²)	X Axis	Y Axis	Z Axis
Set 1	12423.11	2279.76	2434.32
Set 2	3052.56	11650.31	2434.32
Set 3	3052.56	2279.76	11804.87

Table 5.8

Dynamic loads for sandwich panel with aluminum honeycomb as core.

Load Sets (g's)	X Axis	Y Axis	Z Axis
Set 1	33.62	5.90	6.30
Set 2	7.90	31.62	6.30
Set 3	7.90	5.90	32.02
Load Sets (in/sec²)	X Axis	Y Axis	Z Axis
Set 1	12991.53	2279.76	2434.32
Set 2	3052.56	12218.73	2434.32
Set 3	3052.56	2279.76	12373.29

The dynamic loads are in sets of three and it is realized that third load case that has higher load in the Z-axis can cause higher stresses on the panel. Therefore the stress characteristics of the third load set are shown in the Figures 5.5, 5.6, 5.7 and 5.8. The individual face sheet and core stress distribution are also shown. The stresses are then compared to their material ultimate strength for failure and results are tabulated.

5.3.2 Stress Distribution

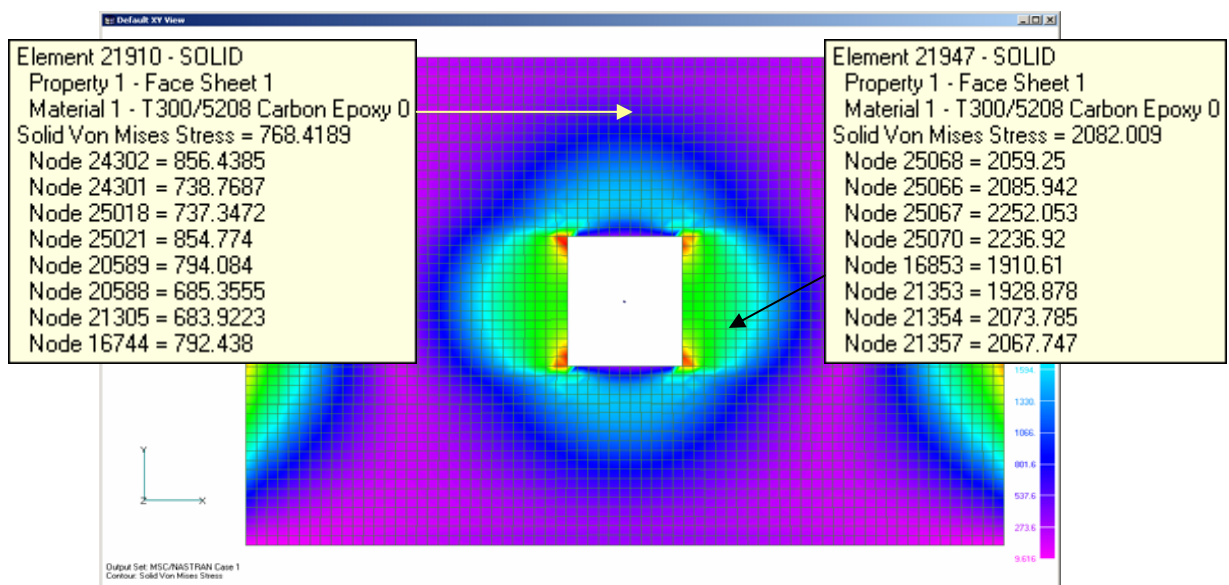


Figure 5.5. VonMises stress distribution of face sheet [0] for launch load set 3.
Inset Element stress located close to cutout and away from the cutout

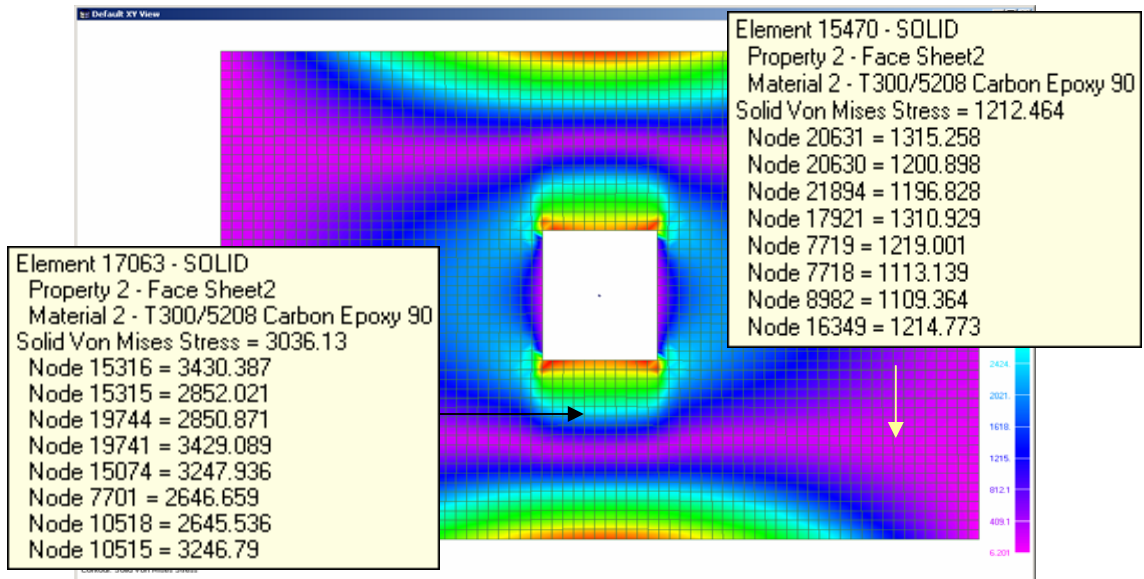


Figure 5.6. VonMises stress distribution of face sheet [90] for launch load set 3.
 Inset Element stress located close to cutout and away from the cutout

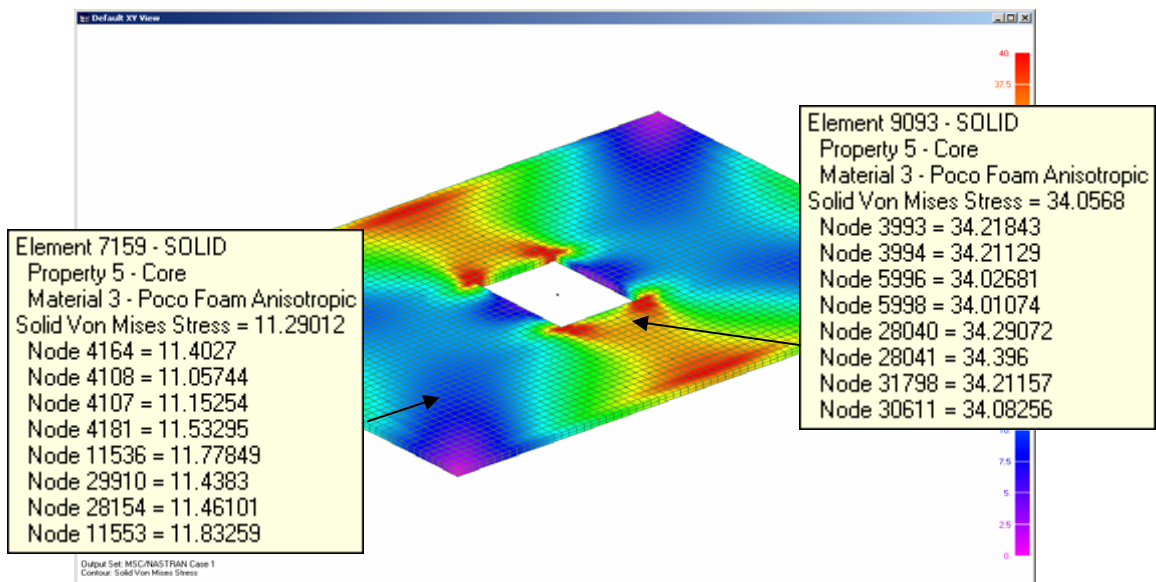


Figure 5.7. VonMises stress distribution of Poco foam core for launch load set 3.
 Inset Element stress located close to cutout and away from the cutout

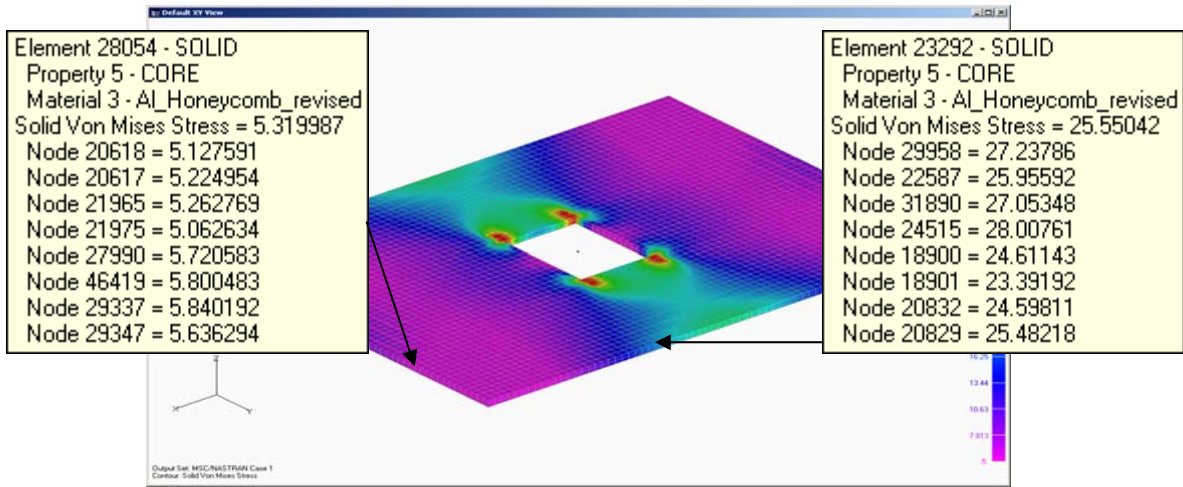


Figure 5.8. VonMises stress distribution of honeycomb core for launch load set 3. Inset Element stress located close to cutout and away from the cutout

Table 5.9

Stress distribution summary.

Dynamic Load Set 3 (VonMises Stresses)	Face sheets (T300/5208 carbon epoxy)		Cores		
	[0] (PSI)	[90] (PSI)	Poco foam (PSI)	Poco foam HTC (PSI)	Aluminum honeycomb (PSI)
Range	(500-4000)	(500-7000)	(10-50)	(10-50)	(10-50)
Element Maximum	5231	9036	63	66	78
Material Allowable	218000 [22]		435 [3]	855 [3]	Compressive strength [32] 195
					Shear Strength [32] 139

The stress distribution summary Table 5.9 indicates that the stresses in the face sheets and the core are well within the limits. Therefore it can be stated that the stresses due to static and dynamic loads will not cause failure to the sandwich radiator panel.

5.4 Heat Transfer Analysis of Radiator Panel

The foremost and important function of this radiator sandwich panel is to dissipate the 100 W/m^2 of heat flux that is generated in the electronics box of the given payload. The method of loading along with environment and edge conditions are discussed in the section 4.6. The section 4.6.4 predicts one-dimensional steady state temperature and stress field and provides approximate numerical results. Now, it is of interest to determine the temperature distribution due to thermal loads supplied to the panel and compare the results with analytical predictions. The panel is first analyzed for steady state heat transfer to predict the temperature response of the radiator panel. The radiator panel with only one side exposed to radiation experiences temperature gradient all along the panel. The temperature gradient coupled with difference in thermal expansion coefficients between the core and face sheets generate thermal stresses due to boundary constraints. The temperature field existing in the face sheets and core is presented in the Figures 5.9, 5.10 and 5.11.

When looking at temperature field, it is readily identified that the face sheets 0 and 90 that are not exposed to radiation, are at higher temperatures than those that are exposed. It is also noted that the core, which receives the heat flux is also at higher temperature when compared to the face sheets. As the face sheets are order of 0.01 inch, temperature difference does not exist between the face sheets. This is also proved by a simple one-dimensional temperature predictions presented in the section 4.6.4. It should be noted that temperature at the surface of the face sheet from one-dimensional calculation is in good agreement with the results from MSC Nastran. It is to be mentioned that temperatures at the elements around the free edges are predicted high compared to the

elements bounded. The temperatures that are presented here represent the elements, which are not affected by the cut out and free edges. The temperature distribution for the face sheets and Poco foam core only are presented and the rest of the temperatures tabulated.

5.4.1 Temperature Distribution

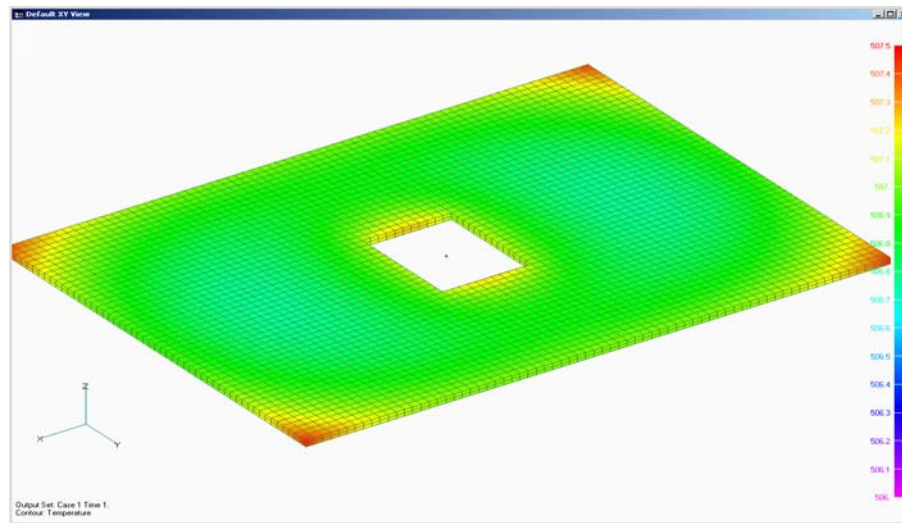


Figure 5.9. Temperature distribution of Poco foam core. (281.5°K)

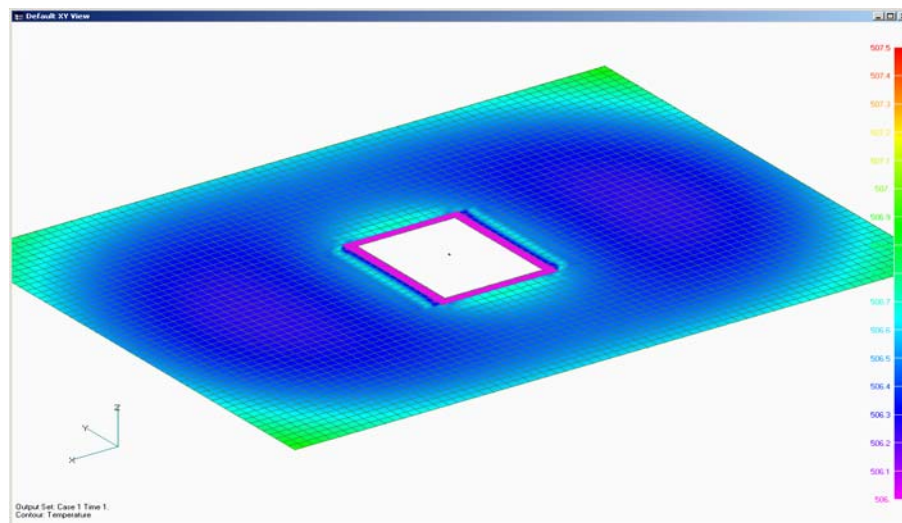


Figure 5.10. Temperature distribution of face sheet [0] exposed to radiation. (281.3°K)

The Figures 5.9 and 5.10 indicate that the temperature difference between the upper most face sheets and the core is negligible. The results of the panel with Poco foam HTC core are similar to the panel with Poco foam core. Therefore the results are not presented. The temperature distribution of aluminum honeycomb core is shown in the Figure 5.11.

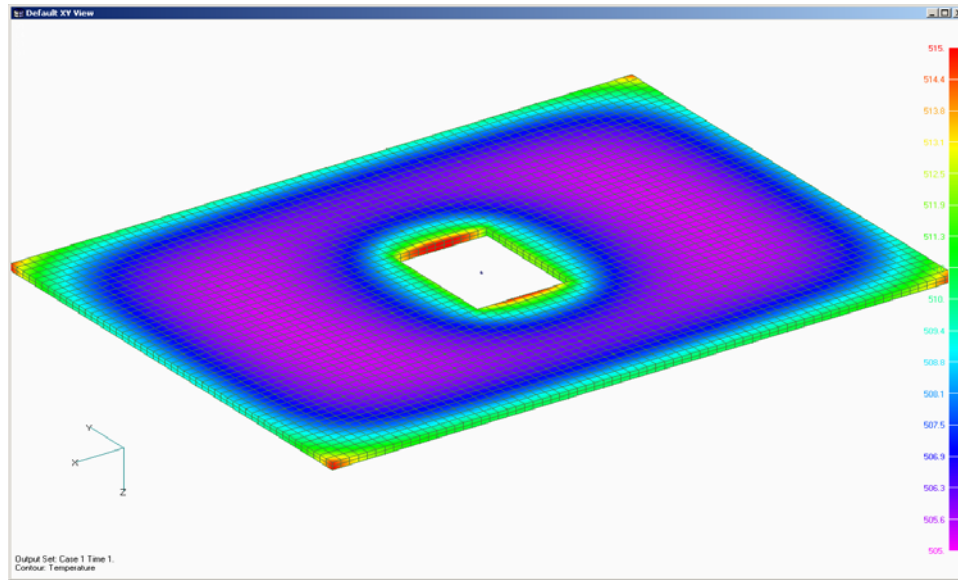


Figure 5.11. Temperature distribution of aluminum honeycomb core. (281.6°K)

The results of steady state heat transfer analysis predicting the temperature distribution in the panel due to heat loads of 100 W/m^2 is tabulated. As proved in the one-dimensional calculation, the Table 5.10 reflects the temperatures of the face sheets and the core with little difference in the temperature field through the thickness.

Table 5.10

Steady state temperature distribution in the radiator panel.

Temperature in Kelvin	Face sheet [0] Exposed to Radiation	Face sheet [0] not exposed to radiation	Poco Foam and HTC core	Aluminum Honeycomb core
Range	(277.8-283.3)	(280.6-284.4)	(281.2-281.9)	(280.7-285)
Element away from edge/cutout	281.4	281.7	281.6	281
Minimum	250	280	280.3	281.1
Maximum	284.4	286.1	282	286.1

5.4.2 Thermal Stress Distribution

The temperature gradient existing in the panel coupled with difference in thermal expansion coefficients between the face sheets and core cause thermal stresses in the panel. These are summarized in the following Table 5.11. They are found to be well within the material allowable that are presented in Table 5.9.

Table 5.11

Thermal stress field in the radiator panel.

Stress in PSI	Face sheet [0]	Face sheet [90]	Poco Foam and HTC core	Aluminum Honeycomb core
Range	(700-1000)	(700-1000)	(1.3-5)	50-120
Element away from edge/ cutout	942	943	3	60
Minimum	490	490	1.3	40
Maximum	1600	1600	5	160

The stress predictions of MSC Nastran are verified using a composite laminate software Laminator [30] which is a two-dimensional Classical Laminate Plate Theory formulation. The maximum temperature gradient found from MSC Nastran is used as thermal load input to the laminator and the corresponding stresses are compared. Care is taken in using the same set of boundary conditions in both the analytical tools to compare the numbers. The stress comparisons are shown in the Table 5.12. The table indicates a very good agreement of Nastran values with Laminator. This comparison is just to validate the results from MSC Nastran.

Table 5.12

Thermal stress comparison with laminator.

Analysis Tool	Components	X Normal Stress	Y Normal Stress
Laminator	Face sheet [0]	1988	-1988
	Face sheet [90]	-1988	1988
	Poco foam core	0.03	0.03
MSC Nastran	Face sheet [0]	1813	-1881
	Face sheet [90]	-1934	1857
	Poco foam core	0.05	0.02

5.4.3 Transient Heat Transfer Analysis

Significant conclusions cannot be made from the steady state heat transfer analysis in regard to the performance of the radiator panel. Although the thermal conductivity of the Poco products are higher than aluminum honeycomb, the performance is not realized in the aspect of temperature field, as the thickness of the panel or the core is small. As discussed in the steady state heat transfer section 4.6.4, and presented in the temperature distribution summary Table 5.10, it is difficult to choose the most suitable core among Poco products and aluminum honeycomb. This is because the temperature field is more or less uniform in all the type of cores. Therefore it is essential to conduct a transient heat transfer analysis on the radiator panel to determine the performance of the cores. As discussed in the transient heat transfer section, it is to be mentioned that transient analysis depends on the material properties such as density and specific heat capacity of the components of radiator. It is known that there is a significant advantage for aluminum honeycomb in terms of density and specific heat capacity. A graph is

presented based on the transient analysis results from MSC Nastran. This is shown in Figure 5.12. This plot does not involve Poco foam HTC as the specific heat capacity is assumed to be same as Poco foam and not much difference exists in density. But parental aluminum material is included just to provide a reference of the behavior of the materials to thermal loads.

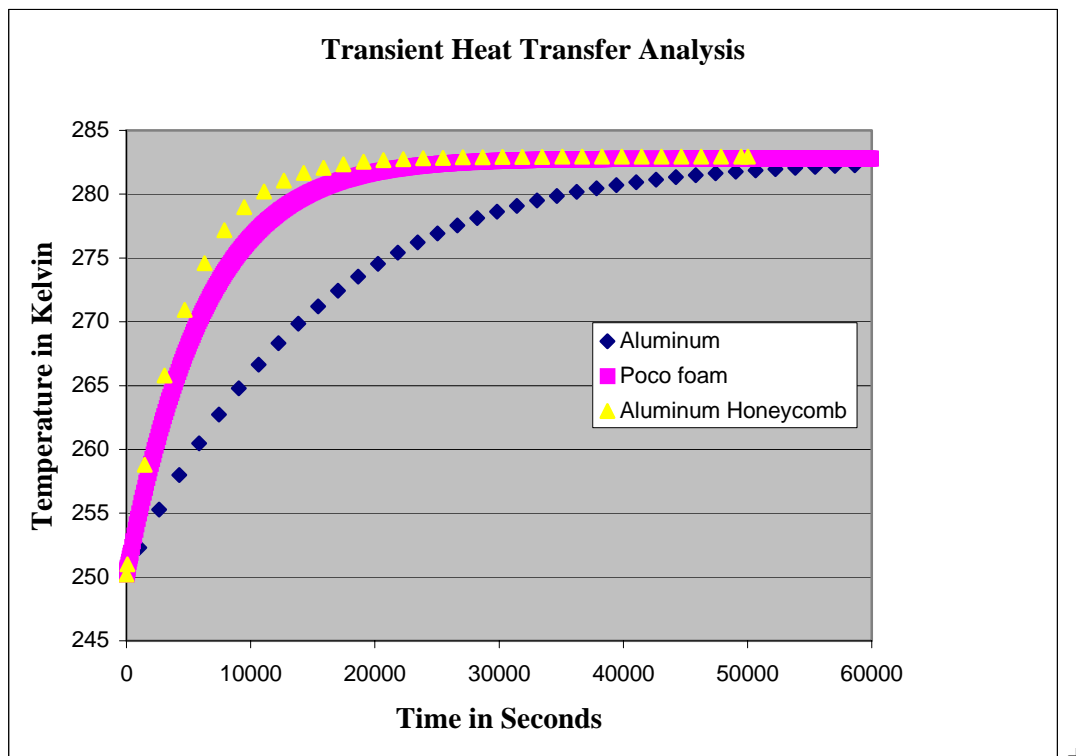


Figure 5.12. Transient temperature plot of a node in core for non-optimized panel from MSC Nastran.

The temperature in the Figure 5.12 is in Kelvin. The steady state temperature for all the three cores lies in the range **(282.5-282.7⁰K)**. This temperature matches well with the steady state temperature output from MSC Nastran. It also indicates that steady state temperature is more or less the same for all the radiator panels with different core materials. But the time it takes to reach the steady state temperature varies based on the

specific heat and density of the material. Although aluminum and aluminum honeycomb have the same specific heat capacity, it differs significantly with density. This can be said that the aluminum panel will take more time to attain steady state. If the Poco foam and aluminum honeycomb curves are considered, it can be noticed that aluminum honeycomb attains stability faster than Poco foam. This can be seen in the following calculation. The time taken to attain steady state for a transient heat transfer problem involving radiation is determined by the equation 5.1.

$$t = \frac{m C_p}{h_i A} \ln \left(1 - \frac{h_i A}{Q} \theta \right) \quad (5.1)$$

The product of mass and specific heat capacity is an important factor to determine the time taken to reach steady state. This along with the total time taken is in the Table 5.13.

Table 5.13

Transient analysis data for different core materials.

Transient Analysis Parameters	Poco foam	Aluminum Honeycomb
m*C_p (J/°K)	17059	15548
Total time (seconds)	60042	50037

This analysis from MSC Nastran is verified by developing a simple mathematical model for transient heat transfer problem involving radiation using Maple software version 8.0 [30]. In this model for calculation purposes, it is assumed that there are no face sheets in the radiator panel. This is a valid assumption because it is already proved in section 4.6.4.1 that face sheets do not contribute much towards heat transfer. The material properties for the Poco foam and aluminum honeycomb are the same used before. The

temperature-time plot, which is shown in the Figure 5.13, has more meaning as it vividly shows a distinction between poco foam and aluminum honeycomb core. This distinction does not exist in the Figure 5.12 because the face sheets are not optimized and therefore the time taken to attain steady state is comparatively higher than shown in Figure 5.13. Although the plot from the Maple in Figure 5.13 does not involve the face sheets, it can be related to that of the plot from MSC Nastran, as the face sheets in the optimized panel are very thin and do not contribute much to the weight.

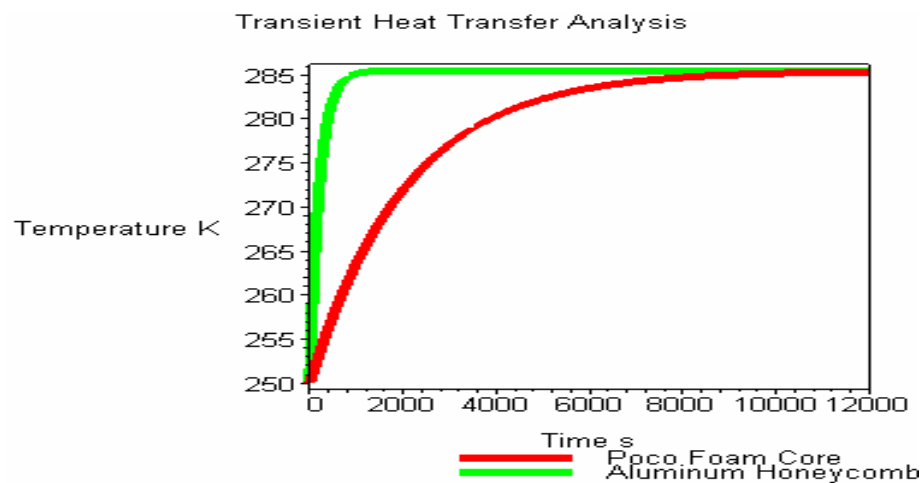


Figure 5.13. Transient temperature plot of core for optimized panel. (assuming no face sheets)

The temperature field in both cores is within the material limits. Therefore both core materials can be a good choice for the core of radiator panel. But it should also be noticed from the Figures 5.12 and 5.13 that at any given point of time before attaining steady state aluminum honeycomb experiences higher temperature than Poco foam.

5.4.4 Orbit Analysis Results

On orbit analysis of the radiator panel is of interest, as the heat received from the sun through radiation cannot be ignored. This analysis is done using Thermal desktop [31].

The parameters and the assumptions of this model are discussed in the section 4.6.7. This study is performed for poco foam and aluminum. It is shown that for a given surface area and mass, poco foam reaches slightly higher temperature than aluminum. It should be noted that this analysis does not include the heat load of 100 W/m^2 from the electronics box. The heat loads for this model are obtained from the sun. The temperature-time plot for the two core materials can be found in the Appendix 2. The Table 5.14 summarizes the results of this analysis.

Table 5.14

Orbit analysis temperature at the core.

Temperature in Kelvin	Poco foam	Aluminum
Maximum Temperature (When facing the sun)	322	315
Minimum Temperature (When not facing the sun)	264	270

The temperatures in the table suggest that not much difference exists between the core materials when facing the sun. But it can be noted based on the surface temperatures, that aluminum honeycomb material can draw more heat from the electronics box assembly. Overall, heat transfer analysis of the radiator panel explores the suitability of the Poco foam and aluminum honeycomb. Based on the results of steady state analysis, it can be only stated that both the core materials satisfy the requirements. But from the transient graphs a clear understanding can be made on the heat extracting abilities of core materials from electronics box assembly. Still it is found difficult to choose the best material for the core because of the fact that the analysis does not reveal the temperature profile of the electronics box. As, much focus is on the rapid removal of heat from the electronics box, the analysis can be concluded with the following distinct approach.

5.4.5 Electronics Box Approach

A comprehensive heat transfer analysis including steady state, transient and on-orbit analysis has been formulated and their results presented. It is to be noted that temperature profile predicted so far is on the radiator side and it is essential to predict the temperature profile of the electronics box after the heat removal. In the heat transfer analysis it is assumed that heat load is applied at the mid-plane of the core and it is dissipated to the surroundings. But in the actual scenario, the heat from the electronics box is carried by a coolant to one edge of the panel and is assumed to pass through tubes existing at the core of the radiator panel. After passing the heat to the core, the coolant is re-circulated to the electronics box for the next cycle. Because of the pipes in the core, there needs to be a temperature gradient along the length of the core. It is well known in such cases that one edge of the core that receives the heat will be at a higher temperature than the other edge. Therefore it is reasonable to make the assumption of adding the heat flux load of 100 W/m^2 at one edge of the core and exposing one of the face sheets to radiation. This approach does not add heat load at one edge but instead attaches the electronics box on one side of the core and heat energy of 100 W is allowed to generate in the electronics box. By this approach the core is needed to extract the heat from the electronics box and dissipate to the surroundings. With this approach it is of interest to know which of the core materials is able to extract more heat from the electronics box and be able to radiate to the surroundings. The temperature profile at the electronics box is plotted against time to find out the steady state temperature and the time required to attain that temperature. The material of the electronics box is assumed to be Beryllium copper alloy. The material property input is shown in Figure 5.14. The dimensions of the electronics box are assumed to be 34 X 1 X 0.6 inches. The material properties are in Nastran units, which are shown in Table 3.1.

Figure 5.14. Material data form for beryllium copper alloy.

The model set up with the representation of the electronics box in MSC Nastran is shown in Figure 5.15.

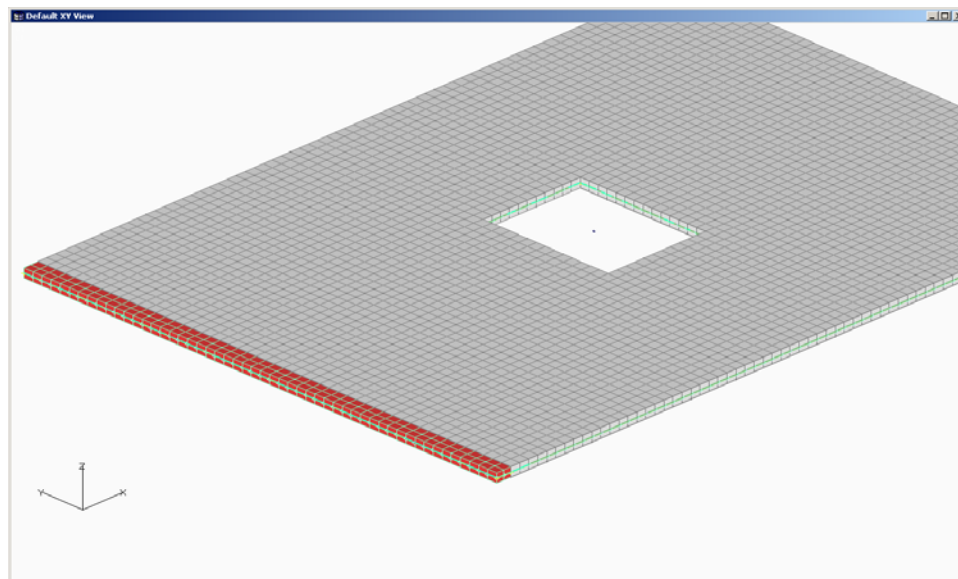


Figure 5.15. Electronics box model set up in MSC Nastran.
Red color represents the electronics box.

The model with the heat generation and radiation is shown in the Figure 5.16. It has the heat generation at the nodes in the electronics box and one side of the panel is exposed to radiation. A transient heat transfer analysis is performed on the model.

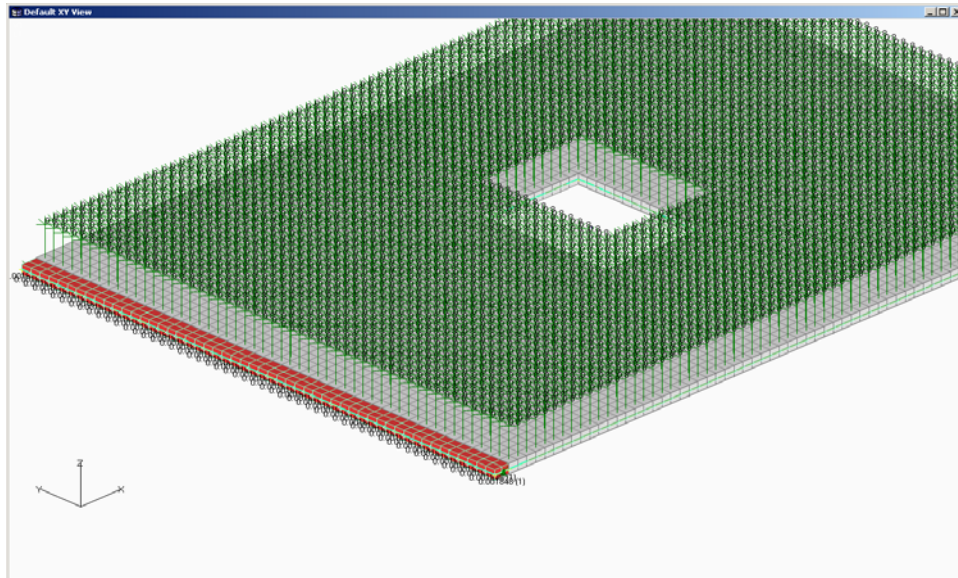


Figure 5.16. Model of electronics box approach with heat generation and radiation.

The time- temperature plot for a node in the electronics box is shown in the Figure 5.17.

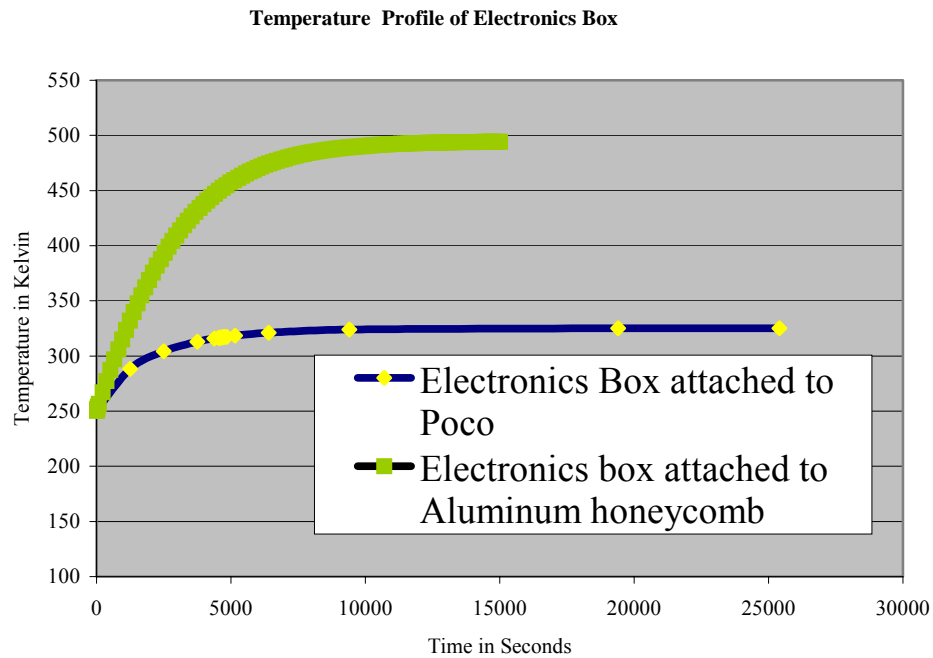


Figure 5.17. Time –temperature plot for a node of the electronics box.

The plot reveals the true potential of Poco foam exhibiting its high thermal conductivity. It provides the fact that thermal conductivity of the core is an important parameter in deciding the temperature profile of the electronics box. The final steady state temperature of the electronics box after the analysis is given in the Table 5.15.

Table 5.15

Steady state temperature of the electronics box.

Material of the core	Steady state temperature at the electronics box (Kelvin)
Poco foam	325
Aluminum Honeycomb	495

The Table 5.15 indicates that the electronics box temperature is maintained very low with Poco foam core. The difference in the electronics box temperature is primarily due to the difference in the in-plane and through the thickness thermal conductivities between the cores.

5.5 Conclusion

To identify the optimum sandwich panel that can act as a radiator for the given payload, satisfying the design requirements, three-dimensional finite element models are developed using MSC Nastran and a comprehensive analysis is performed and the results presented. The optimum lay-up and orientation is carefully determined with the chosen material properties satisfying the vibration and static requirements. The modes, stress and temperature predictions using MSC Nastran is verified by developing simple analytical models that represents the radiator problem with certain assumptions. The analytical model results correlate well with MSC Nastran.

In addition steady state and transient heat transfer analysis of the radiator panel explores the thermal characteristics of the core materials identified. In all the cores the temperature profile is more similar to one another with the given boundary conditions. Furthermore, to realize the potential thermal performance of the radiator, a distinct approach to find the temperature profile of the electronics box is put forth. The temperature of the electronics box predicted with aluminum honeycomb core is reduced with embedded heat pipes all along the core. This increases the weight, cost and complexity of the radiator panel compared to a core of Poco graphite foam. This approach illustrates that out of the core materials investigated, Poco foam is capable of removing the heat rapidly and maintaining a low temperature profile in the electronics box with reduced cost and complexity. Therefore the radiator panel for the given payload will have Poco foam as its core material.

REFERENCES

- [1] McHugh S. LAT Radiator finite element structural vibration analysis. GLAST LAT-TD-00491-1, 2001.
- [2] Teti NM. EO-1 technology transfer report for the carbon/carbon radiator. Swales Aerospace NASA/GSFC, 2001.
- [3] Poco Graphite Incorporation company website, accessed 2003, <<http://www.pocothermal.com/>>.
- [4] MSC Software Corporation company website, accessed 2003, <http://www.mssoftware.com/support/prod_support/nastran/>.
- [5] Vinson JR. Behavior of sandwich structures of isotropic and composite materials. Lancaster Pa: Technomic Publication; 1999.
- [6] Composite materials design online course website, accessed 2003, <<http://callisto.my.mtu.edu/my4150/sandwich/sp1.html>>.
- [7] Harris RH, Rais-Rohani M. Analysis and design optimization of composite sandwich plates under axial and biaxial in-plane loads, SECTAM XVIII Conference, Tuscaloosa, Alabama, 1996.
- [8] Klett J. High thermal conductivity, mesophase pitch derived carbon foams, Oak Ridge National Laboratory, Tennessee, 1999.
- [9] Klett J, Conway B. Thermal management solutions utilizing high thermal conductivity graphite foams. SAMPE Symposium and Exhibition, Long Beach, California, 2000.
- [10] Whitney JM, Pagano NJ. Shear deformation in heterogeneous anisotropic plates. ASME J Appl Mech 1970;37(4):1031-6.
- [11] Reddy JN. Free vibration of antisymmetric angle ply laminated plates including transverse shear deformation by the finite element method. J Sound Vibration 1979;4:565-76.
- [12] Sun CT, Whitney JM. Theories for the dynamic response of laminated plates. AIAA J 1973;11:178-83.

- [13] Noor AK, Burton WS. Stress and free vibration analysis of multiplayer composite plates. *Compos Struct* 1989;11:183-204.
- [14] Kant T, Swaminathan K. Analytical solutions for free vibration of laminated composite and sandwich plates based on a higher order refined theory. *Compos Struct* 2001;53:73-85.
- [15] Pandya BN, Kant T. A consistent refined theory for flexure of a symmetric laminate. *Mech Res Commun* 1987;14:107-13.
- [16] Reddy JN. A simple higher order theory for laminated composite plates. *ASME J Appl Mech* 1984;51:745-52.
- [17] Reddy JN, Phan ND. Stability and vibration of isotropic and laminated plates according to higher order shear deformation theory. *J Sound Vibration* 1985;98:157-70.
- [18] Ochoa OO, Engblom JJ, Tucker R. A study of the effects of kinematic and material characteristics on the fundamental frequency calculations of composite plates. *J Sound Vibration* 1985;101(2):141-148.
- [19] Ochoa OO, Walsh TJ. Composites with multiple cutouts. *Compos Struct* 1993;24:117-124.
- [20] Swann TR. Heat transfer and thermal stresses in sandwich panels. NACA TN-4349, 1958.
- [21] MSC Nastran for windows quick start guide, 1995.
- [22] Carbon/graphite composite material database website, accessed 2003, <<http://plastics.about.com/library/data/blcarbon.htm>>.
- [23] Knight M. Three-dimensional elastic properties of carbon/epoxy composites. *J Comp Materials* 1982;16:153-159.
- [24] Hilton HH, Yi S. Stochastic delamination simulations of nonlinear viscoelastic composites during cure. *J Sandwich Struct and Materials*. 1999;1:111-127.
- [25] Cheng J. Thermal shape change of some CFRP- aluminum honeycomb sandwiched structures. *SPIE* 2002;4837:336-341.
- [26] HEXCEL composites company website, accessed 2003,

- <http://www.Hexcelcomposites.com/Markets/Products/Honeycomb/Hexweb_attrib>
- [27] Gilmore DG. Satellite thermal control handbook. The Aerospace Corporation press, El Segundo, California, 1994.
- [28] Maplesoft company website, accessed 2003,
<<http://www.maplesoft.com/>>.
- [29] Whitney JM. Structural analysis of laminated anisotropic plates. Lancaster Pa: Technomic Publication; 1987.
- [30] The Laminator official website, accessed 2003,
<<http://thelaminator.net/>>.
- [31] Thermal Desktop Version 4.4 User's Manual, 2001.
- [32] Aluminum honeycomb core strength properties website, accessed 2003,
< http://www.plascore.com/5056_2.htm>.
- [33] Reddy JN. Mechanics of laminated composite plates: theory and analysis. Boca Raton: CRC Press, c1997.

When you use the MAT9 entry, it is advisable to define a material coordinate system on the PSOLID entry (using field 4). For solid elements, stresses are output in the material coordinate system, which by default, is the basic coordinate system. In general, for solid elements, it is not easy to determine the orientation of the element coordinate system.

If you want to use the MAT9 entry to define an orthotropic material, the terms of the material matrix $[G]$ can be generated by using Eq. (5-9):

$$\begin{aligned}
 G_{11} &= \frac{1 - \nu_{yz}\nu_{zy}}{E_y E_z \Delta} & G_{12} &= \frac{\nu_{yx} + \nu_{zx}\nu_{yz}}{E_y E_z \Delta} & G_{13} &= \frac{\nu_{zx} + \nu_{yx}\nu_{zy}}{E_y E_z \Delta} \\
 G_{22} &= \frac{1 - \nu_{xz}\nu_{zx}}{E_x E_z \Delta} & G_{23} &= \frac{\nu_{zy} + \nu_{xy}\nu_{zx}}{E_x E_z \Delta} & & \\
 G_{33} &= \frac{1 - \nu_{xy}\nu_{yx}}{E_x E_y \Delta} & & & &
 \end{aligned} \tag{5-9}$$

where ν_{ij} = Poisson's ratios

E_x, E_y, E_z = Young's modulus in the x-, y- and z-directions

G_{xy}, G_{yz}, G_{zx} = shear moduli

$$\Delta = \frac{1 - \nu_{xy}\nu_{yx} - \nu_{yz}\nu_{zy} - \nu_{xz}\nu_{zx} - 2\nu_{yx}\nu_{zy}\nu_{xz}}{E_x E_y E_z}$$

also $G_{44} = G_{xy}$

$G_{55} = G_{yz}$

$G_{66} = G_{zx}$

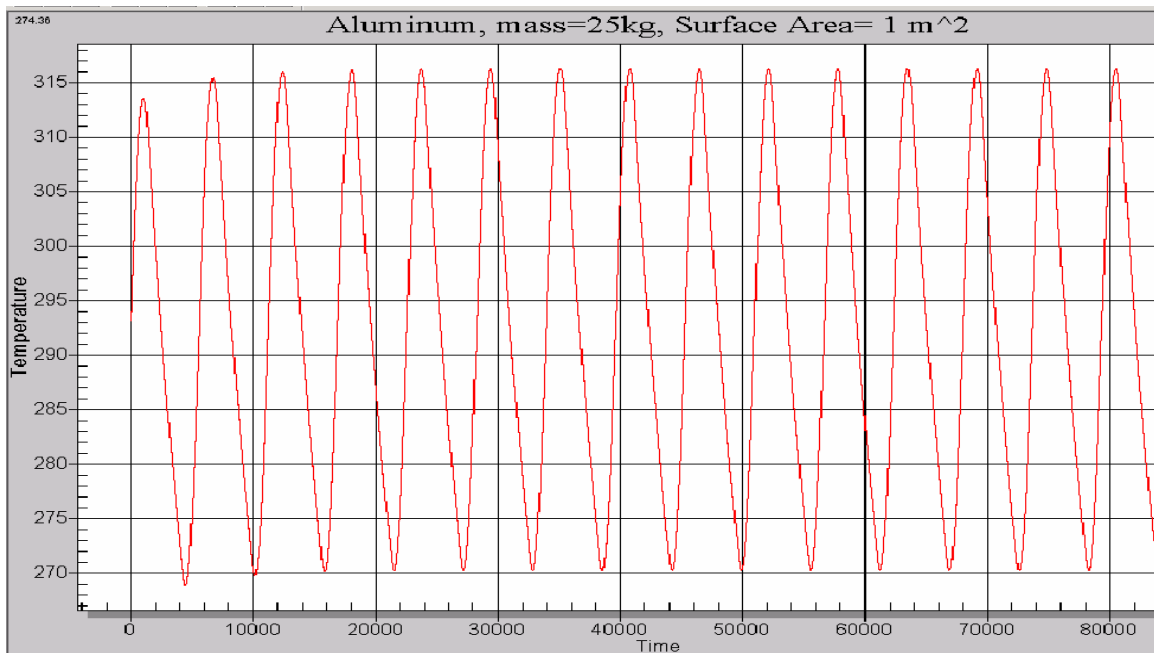
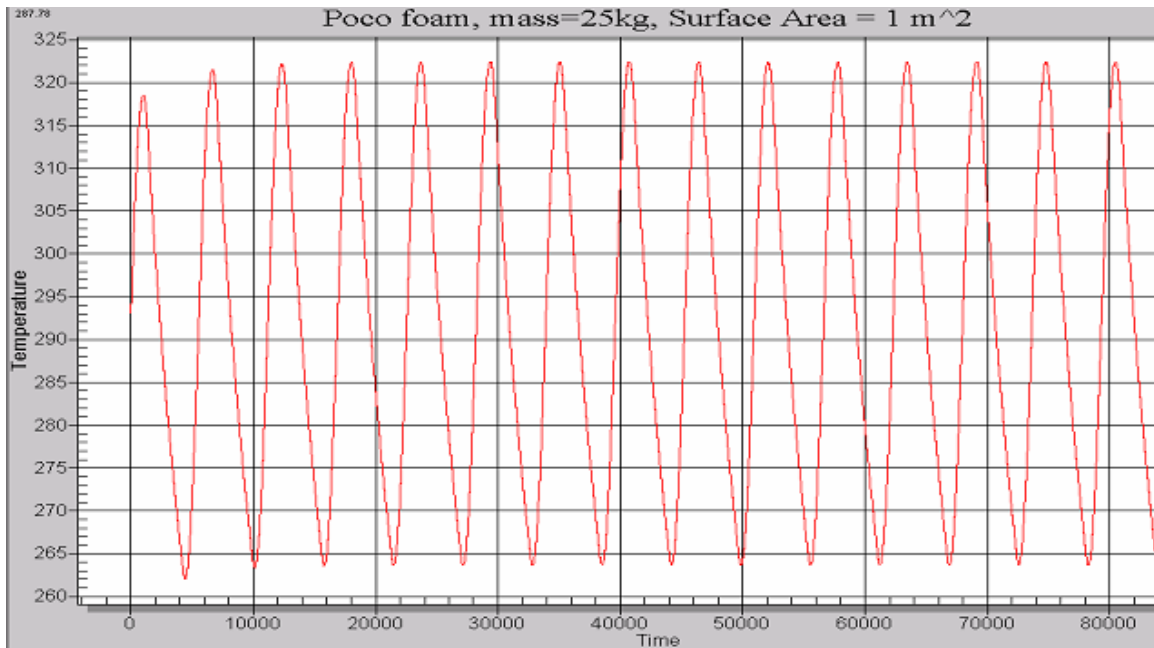
and $G_{14} = G_{15} = G_{16} = 0.0$

$G_{24} = G_{25} = G_{26} = 0.0$

$G_{34} = G_{35} = G_{36} = 0.0$

$G_{45} = G_{46} = G_{56} = 0.0$

APPENDIX 2



APPENDIX 3

Elastic Properties [25] calculation for aluminum honeycomb is given by the following equations.

$$E_L = \frac{3 * t_c * E_{aluminum}}{10 * d_c}$$

$$E_W = \frac{t_c * d_c * E_{aluminum}}{3 * l_c^2}$$

$$E_Z = \frac{4 * t_c * E_{aluminum}}{3 * d_c}$$

Where l_c is the length of the core and t_c is the thickness of the core. And $d_c = 0.866 * l_c$.

Young's Modulus of Aluminum 6061 is given by

$$E_{aluminum} = 10E07 \text{ Psi}$$

Substituting $l_c = 46$ inches and $t_c = 0.6$ inch, the parameter d_c is calculated to be 39.836 inches, the young's modulus in the L (X), W (Y) and Z directions are calculated to be as follows.

$$E_L = 4.52 \text{ E04 Psi (0.31 Gpa)}$$

$$E_W = 3.76 \text{ E04 Psi (0.26 Gpa) and}$$

$$E_Z = 2.01E05 \text{ Psi (1.39 Gpa)}$$

The shear modulus [1] is assumed to be as follows.

$$G_{12} = G_{13} = 0.1 \text{ Gpa and } G_{23} = 0.40 \text{ Gpa.}$$

The effective thermal Conductivity for aluminum honeycomb for L (X), W (Y) and Z directions are calculated as follows

$$K_x = \frac{K_{aluminum} \delta}{S}$$

$$K_y = \frac{3}{2} \frac{K_{aluminum} \delta}{S}$$

$$K_z = \frac{8}{3} \frac{K_{aluminum} \delta}{S}$$

The aluminum honeycomb core used in the analysis has a foil thickness, δ , of 0.001 inches and nominal cell dimension, S of 0.25 inches [26]. The thermal conductivity of aluminum 6061 ($K_{aluminum}$) is 1160 Btu-in/hr-ft²-°F.

VITA

Sudharsan Mukundan was born in India. He obtained his Bachelor of Engineering degree (with distinction) in mechanical engineering from Barathiar University, Coimbatore, India in April 2001. Upon completion of his master's, he plans to gain work experience in the field of design and finite elements.

His permanent address is:

Plot No. 81, II Main Road,

South Jagannatha Nagar,

Villiwakkam,

Chennai, (TN) - 600049.

India.

Phone: (91)-44-26174283

E-mail: shudh@tamu.edu

adharsh78@hotmail.com